Dark Matter Particle in QCD

Glennys R. Farrar, Zihui Wang (王子汇), and Xingchen Xu (许星辰)

Center for Cosmology and Particle Physics, Department of Physics, New York University, NY, NY 10003, USA

(Dated: July 22, 2020)

We report on the possibility that the Dark Matter particle is a stable, neutral, as-yet-undiscovered hadron in the standard model. We show that the existence of a compact color-flavor-spin singlet $uuddss$ (Sexaquark, S) with mass of order $2\,m_p$ is compatible with current knowledge and that, if it exists, the S is a very attractive DM candidate. The S interacts with baryons primarily via a Yukawa interaction of coupling strength α_{SN}, mediated by exchange of the flavor-singlet superposition of the ω and ϕ vector mesons, denoted V, having mass ≈ 1 GeV. We emphasize the need to distinguish between S-nucleon scattering amplitudes which are of a hadronic scale, and S breakup amplitudes which are dynamically suppressed and many orders of magnitude smaller, akin to the weak interaction level. We use SNOlab and other data to obtain the most stringent constraints on the effective vertex for breakup, $\tilde{g}$, from the stability of DM and nuclei. The relic abundance of S Dark Matter (SDM) is established when the Universe transitions from the quark-gluon plasma to the hadronic phase at ≈ 150 MeV and is in remarkable agreement with the observed $\Omega_{DM}/\Omega_b = 5.3 \pm 0.1$; this is a no-free-parameters result because the relevant parameters are known from QCD. Survival of this relic abundance to low temperature requires $\tilde{g} \lesssim 2 \times 10^{-6}$, comfortably compatible with theory expectations and observational bounds. To analyze bounds on SDM we must solve the Schroedinger equation to determine the cross section, σ_A, for S scattering on nucleus A. Depending on α_{SN}, the true cross section can be orders of magnitude larger or smaller than given by Born approximation; this requires a reanalysis of observational limits. We use direct detection experiments and cosmological constraints to determine the allowed region of α_{SN} for the mass range relevant to SDM. If the S-nucleon interaction is attractive and strong enough, DM-nucleus bound states will form. For a range of allowed values of α_{SN}, we predict exotic nuclear isotopes at a detectable level with mass offset ≈ 2 amu. Dedicated study of this mass-offset range, for a wide range of elements, is warranted. We argue that the neutron-star equation of state and SN1987a cooling are not constraining at this time, but could become so in the future when better understood. Finally, we discuss strategies for detecting the sexaquark in accelerator experiments. This is surprisingly difficult and experiments to date would not have discovered it. The most promising approaches we identify are to search for a long-interaction-length neutral particle component in the central region of relativistic heavy ion collisions or using a beam-dump setup, and to search for evidence of missing particle production characterized by unbalanced baryon number and strangeness using Belle-II or possibly GLUEX at J-Lab.

I. INTRODUCTION

A successful model for dark matter (DM) must predict the observed relic DM density and ideally also provide a natural explanation for the observed DM to baryon ratio, $\Omega_{DM}/\Omega_b = 5.3\pm 0.1$ [1]. It must be compatible with cosmological and astrophysical constraints on structure formation and DM interactions and not alter or interfere with the successful predictions of primordial nucleosynthesis. The DM interactions with normal matter must also satisfy direct detection bounds and constraints from laboratory and geophysical experiments, and must be compatible with observed properties of galaxies, neutron stars, white dwarfs, supernovae, and other astrophysical objects.

We show here that the sexaquark S – a conjectured neutral, color-flavor-spin-singlet bound state of six light quarks $uuddss$ with mass $m_S \approx 2m_p$ – satisfies or is compatible with all of the above criteria given present limits to our understanding. For $m_S < m_D + m_e$ the S is absolutely stable and for $m_S \lesssim 2$ GeV its lifetime is greater than the age of the Universe. The potential existence of this state and its compatibility with accelerator experiments was discussed in [2], where it was called sexaquark, adopting the Latinate prefix to dis-

tinguish it from the relatively loosely bound H-dibaryon proposed by Jaffe [3] and the term hexaquark which is a generic term for a 6-quark or $(q\bar{q})^3$ state; S is also a reminder that it is a strange, scalar, flavor singlet.

The relic abundance of sexaquark DM (SDM) follows from general arguments of statistical physics and known standard model parameters – the quark masses and the temperature of the transition from quark-gluon to hadronic phases – and is predicted to be $\Omega_{DM}/\Omega_b \approx 5$ [4], in remarkable agreement with the observed value $\Omega_{DM}/\Omega_b = 5.3 \pm 0.1$ [5]. Preservation of this abundance ratio as the Universe cools requires that the rate for breaking up S's in hadronic collisions be less than the expansion rate of the Universe. This condition is satisfied if the effective Yukawa vertex for breakup $\tilde{g} \lesssim$ few 10^{-6} [4]; this small value naturally follows from the low probability of fluctuation between di-baryon and sexaquark configurations [6] as discussed further in Sec. IV. For future reference, the mean number density of SDM is about 2.5 times that of baryons, since $m_S \approx 2m_p$.

The organization of this paper is the following. In Sec. II we briefly review the particle physics of the proposed S. Then in Sec. III we give the DM abundance analysis predicting $\Omega_{DM}/\Omega_b \approx 5$ in the SDM scenario at freezeout. In Sec. IV we discuss theoretical estimates of the breakup amplitude $\tilde{g}$, and provide improved observational limits as a function of sexaquark mass based on deuteron and sexaquark stability and other constraints. With these basics in place, we proceed

to the other requirements of a successful DM model starting with SDM-matter interactions. The primary coupling of the S to other hadrons is through exchange of the flavor-singlet superposition of the nonet vector mesons, whose mass is of order 1 GeV. The resulting Yukawa interaction between SDM and baryons is non-perturbative over important parts of the relevant parameter range, so the Schroedinger equation must be solved numerically to find the cross sections; this is discussed in Sec. V. Using the exact non-perturbative treatment, in Sec. VI we derive the constraints on the Yukawa interaction strength α_{SN} implied by direct detection experiments, cosmology and astrophysics. The limits are drastically different than would be deduced using Born approximation. In Sec. VII we investigate the self-interactions of SDM and show that the maximum SIDM cross section is $\sigma/m \approx 0.2$ which is lower than generally considered astrophysically useful. Next, in Sec. VIII, we discuss the possible formation of exotic isotopes in which a sexaquark binds to a nucleus, and the constraints which can be placed on the parameter space from those considerations. We find that for an interesting range of currently-allowed parameters there can be a sufficient density of exotic isotopes to be detectable, albeit requiring a new, dedicated search because previous limits are not sensitive to the ≈ 2 amu splitting. Section IX discusses ways to search for sexaquarks in accelerator experiments. Sec. X gives a concise summary of the results of the paper, and we close with conclusions in Sec XI. The Supplemental Material provide additional information on secondary topics.

II. STABLE SEXAQUARK HYPOTHESIS

The stable sexaquark hypothesis [2] postulates that the Q=0, B=+2, $uuddss$ flavor-singlet scalar bound state (denoted S) is stable. The S is absolutely stable if $m_S \leq m_D + m_e = 1876.12$ MeV. A somewhat higher mass can also effectively be stable, because up to $m_S = m_p + m_e + m_\Lambda = 2054.5$ MeV the S decays through a doubly-weak interaction and its lifetime may be longer than the age of the Universe [6]. Both cases are called "stable" below for conciseness. The S cannot be too light, or nuclei would decay. These constraints are discussed in greater detail in Sec. IV.

The stable sexaquark hypothesis is motivated by the unique symmetry of the $uuddss$ ground state. Models designed to fit known hadrons cannot be trusted to reliably describe it because Fermi statistics prevents mesons and baryons from enjoying the triply-singlet configuration (in color, flavor, spin) accessible to $uuddss$. Hyperfine attraction is strongest in singlet configurations, c.f., the Most-Attractive-Channel hypothesis [7], so binding is maximal in the sexaquark channel.

Lattice studies are not yet capable of determining the mass spectrum of the $uuddss$ system. A nearly unbound state is predicted by HAL-QCD [8], a lattice-inspired approach to modeling the physical light quark mass limit which however has been criticized [9, 10]. The NPLQCD group using 850 MeV u, d, s quarks found 80 MeV binding energy in the H-dibaryon channel. Rigorous lattice treatment of a 6-quark system, for physical quark masses, large volume and statistical

sensitivity adequate to be sensitive to the presence of multiple states is extremely challenging and may be many years away. It should be emphasized that there is no incompatibility between the existence of a deeply bound stable S and a loosely bound di-Λ molecule analogous to the deuteron, for which there may be hints in the recent femtoscopy study by ALICE[11]. The presence of such a loosely bound di-Λ would complicate lattice QCD attempts to isolate an orthogonal, deeply bound state.

If it exists, the S should be much more compact and weakly coupled than normal hadrons due to being a flavor singlet and thus not coupling to pions. Baryons ($r_N = 0.9$ fm) are much larger than their Compton wavelength ($\lambda_N = 0.2$ fm), which can be attributed to baryons coupling to pions ($\lambda_\pi = 1.4$ fm). Estimating

$$r_S = \lambda_S + b\lambda_{M1} \tag{1}$$

with $0 \leq b < 0.45$ by analogy with baryons, where $M1$ is the lightest well-coupled flavor singlet meson, presumably the flavor-singlet combination of $\omega - \phi$ with $m_{M1} \sim 800 - 1000$ MeV, gives $r_S = 0.1 - 0.3$ fm.

The disparate size of S and baryons means amplitudes for breakup and formation reactions involving overlap of S and two baryons, are very suppressed; see Sec. IV below for more details. Amplitudes for S-nucleon scattering should be smaller than hadronic scattering amplitudes like NN, πN, etc., due to the absence of pion exchange, but this is less dramatic phenomenologically because the flavor singlet vector meson contribution remains.

Initial searches for a $uuddss$ bound state were stimulated by Jaffe's MIT bag model estimate of 2150 MeV [3] for a state he called H-dibaryon. With a mass below $2m_\Lambda = 2230$ MeV, the state is strong-interaction stable and was almost universally assumed to have a typical weak lifetime $\gtrsim 10^{-10}$ s as a result of expecting $m_H > m_p + m_\Lambda = 2054$ MeV. Additionally, the H was envisaged structurally as a loosely-bound di-Λ, readily formed in hypernuclei, e.g., [12]. Dozens of experiments were performed attempting to find an H-dibaryon, and seem to exclude the original proposal of a di-Λ bound by $\mathcal{O}(100 \text{ MeV})$.

A careful re-examination of the experimental situation by one of us (GRF) showed that no experiment to date would have detected a compact, stable S [2] . Experiments either required $m_H > 2$ GeV, or searched for a signal in the invariant mass of decay products such as $\Lambda p \pi^-$, or implicitly assumed a dibaryon spatial configuration comparable to a deuteron or nucleon so its interactions and production was expected to be comparable to ordinary hadrons; see [2] for further discussion.

If a stable S exists, it could be the Dark Matter particle. Limits on DM-baryon interactions from direct detection experiments, the CMB power spectrum and the indirect limits of [13] from HST orbital decay and evaporation of liquid cryogens, and thermal conductivity of the Earth, are discussed in Sec. V below; these limits prove to be only mildly restrictive on the natural parameter space.

III. DARK MATTER RELIC ABUNDANCE

A. QCD phase transition

At high temperature, the QCD sector consists of a plasma of massless gluons, nearly massless $u, \bar{u}, d, \bar{d}$ quarks and somewhat heavier $s, \bar{s}$ quarks. At low temperature, the QGP is replaced by the chiral-symmetry-broken, color-confined phase in which baryons are heavy and pseudoscalar mesons are light. Lattice QCD calculations show that the transition between the QGP and the low temperature hadronic phase is a cross-over centered on 155 MeV [14] rather than a true phase transition. As the temperature drops from 170 MeV to 140 MeV, the quark and gluon condensates responsible for hadron masses and color confinement increase; at the same time it becomes more favorable energetically for $q\bar{q}$'s and qqq to combine into color singlet mesons and baryons. Typical intra-$q, \bar{q}, g$ separations are $\mathcal{O}(1\,\mathrm{fm})$ for $T \approx 150$ MeV. The age of the Universe in this epoch is $t_{\mathrm{Univ}} = 7.3 \times 10^{-5}(100\,\mathrm{MeV}/T)^2$ sec, whereas the timescale for hadronic interactions is $\mathcal{O}(10^{-23}\mathrm{s})$.

The equilibrium number density of each fermion species as a function of temperature is given by

$$n(m,T) = \frac{g}{2\pi^2} \int_m^\infty \frac{E\sqrt{E^2 - m^2}}{e^{(E \mp \mu)/T} + 1}\, dE, \qquad (2)$$

where $g = 6$ is the number of color-spin degrees of freedom per q and $\bar{q}$ flavor) and μ is the chemical potential.

The quark masses are accurately known from the hadron spectrum in lattice QCD [15]: $m_u = 2.118(38)$ MeV, $m_d = 4.690(54)$ MeV and $m_s = 92.52(69)$ MeV. In the QGP, the relative abundances of photons, gluons, and light quarks $u, \bar{u}, d, \bar{d}$ are in the ratios $1{:}8{:}\frac{9}{4}$, and s quarks have a slightly lower abundance. These flavor ratios apply both to the thermal $q\bar{q}$ quarks and the "baryon excess" quarks. The Baryon Asymmetry of the Universe today, $\eta_0 \equiv n_b/n_\gamma = (5.8 - 6.5) \times 10^{-10}$ (95%CL) [5] amounts to a roughly part-per-billion difference between the q and $\bar{q}$ abundance for each light flavor; to excellent approximation the chemical potential can be ignored for calculating abundances above 100 MeV. Below the hadronization transition, the most abundant particles besides photons and leptons are pions. Weak interactions maintain flavor chemical equilibrium, and hadronic and EM reactions like $\pi^+\pi^- \leftrightarrow \gamma\gamma$ keep hadron abundances in thermal equilibrium well into the low temperature phase.

B. Dark Matter abundance: Ω_{DM}/Ω_b

The microphysics of the QGP to hadron transition is not amenable to detailed calculation, but statistical physics determines the relative occupation of states of different energies at any given temperature. Thus we can estimate the relative abundance of states giving rise to sexaquarks and to anti-sexaquarks, and those giving rise to baryons and anti-baryons, at any given temperature. There are, in addition, other quark, anti-quark and gluonic states which give rise to mesons but
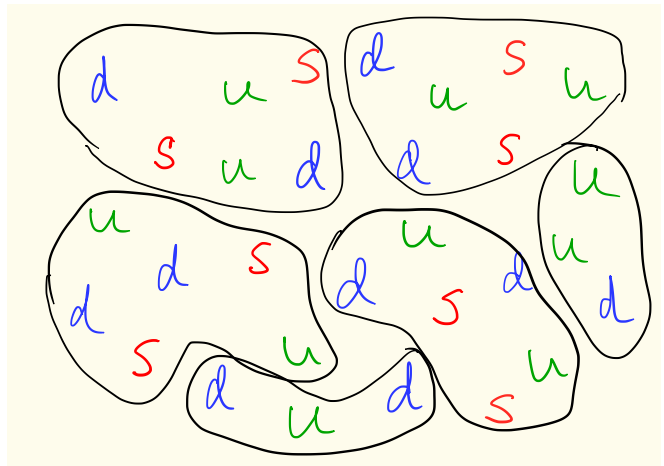

FIG. 1: Schematic illustration of how the deficit of s quarks relative to u, d quarks, $\approx 15\%$ at the transition temperature, leads to residual baryons.

those are not our interest. We speak below of sexaquarks and baryons, but the story is the same for their anti-particles; as noted above, at these temperatures the baryon-anti-baryon asymmetry is almost negligible.

In the SDM scenario, DM consists of sexaquarks containing 2 each of u, d, s quarks. Simply due to their higher mass, the equilibrium fraction of strange quarks and antiquarks, $f_s \equiv (n_s + n_{\bar{s}})/\sum_{i=1}^{3}(n_i + n_{\bar{i}})$ is lower than that of up and down quarks and antiquarks. Over the relevant temperature range, 140-170 MeV, the fraction of s quarks in thermal equilibrium varies from 30-31% with the remaining 70-69% being equally u, d.

If every s in the quark-gluon plasma were in a sexaquark and baryons were only formed from the left-over u, d quarks, the density of S's would be $\frac{f_s}{2} n_q$, where f_s is the fraction of quarks that are s's and n_q is the total density of quarks; the density of baryons would be $\frac{(1-3f_s)}{3} n_q$. As the temperature drops from 170 to 140 MeV, $3f_s$ changes only slightly, from 0.964 to 0.948.

Not every strange quark is in a sexaquark, so we introduce κ_s, the efficiency with which s quarks are trapped in sexaquarks. Thus we have

$$\frac{\Omega_{DM}}{\Omega_b} = \frac{y_b\, \kappa_s\, 3f_s}{1 - \kappa_s\, 3f_s}\,, \qquad (3)$$

where $y_b \equiv m_S/(2m_p)$ is near 1.

We can estimate κ_s as follows. First consider production of S's. Even at the level of 1-gluon exchange, which provides a good qualitative accounting of most hadron mass splittings [16], there is a strong hyperfine attraction between $uuddss$ quarks in the sexaquark (color-, flavor- and spin-singlet) configuration [3, 7]. This perturbative attraction is present independently of whether the quarks are in an isolated, zero-temperature S particle, quark nuggets, or are in the QGP. Thus when the strongly attractive sexaquark configuration of quarks occurs by chance in some spatial region of the QGP, it will be energetically favored and linger in that state. Quarks in con-

figurations which are not energetically favored will continue their random rearranging.

Because the chemical potential is negligible, statistical physics tells us that the relative probability of finding two s quarks in an S-like state compared to finding them in a state consisting of two separate (hyperon-like) 3-quark states, is $\exp(\Delta E)/T$ where ΔE is the energy splitting of the two configurations. When hadronization occurs, the S-like color singlet states become S's and other color singlets become mesons, baryons and anti-baryons; configurations which are not color singlets continue rearranging and form new color-singlet combinations which then become hadrons.

We can estimate ΔE and hence κ_s using physical masses of nucleons, hyperons and the hypothesized mass of the S; this approximation gives

$$\kappa_s(m_S, T) = \frac{1}{1 + (r_{\Lambda,\Lambda} + r_{\Lambda,\Sigma} + 2r_{\Sigma,\Sigma} + 2r_{N,\Xi})} \quad (4)$$

where $r_{1,2} \equiv \exp[-(m_1 + m_2 - m_S)/T]$ and the coefficients of the different terms are the number of combinations of the given baryon states containing $uuddss$. The leading uncertainty due to confinement and chiral-symmetry breaking cancels, to the extent that the presence or absence of the quark and gluon condensates shifts the masses of the S and octet baryons together.

Idealizing the production of DM as occurring at a single effective temperature somewhere in the 140-165 MeV range, and using Eq. (4) to calculate $\kappa_s(m_S)$, leads to the values of Ω_{DM}/Ω_b shown in Fig. 2. The predictions are within a factor-2 of the measured ratio $\Omega_{DM}/\Omega_b = 5.3 \pm 0.1$ over the entire plane. The mild dependence of Ω_{DM}/Ω_b across Fig. 2 follows from the fact that f_s and κ_s have the opposite behavior as T changes, so the product $\kappa_s f_s$ entering Eq. (3) varies relatively little, making the prediction robust to uncertainties in $T_{\rm eff}$. Thus the observed ratio of DM and baryons is a very robust consequence at the $\mathcal{O}(1)$ level of the sexaquark DM model. It is noteworthy that an analogous Freezeout Approximation treatment of nucleosynthesis in central Relativistic Heavy Ion Collisions gives an excellent accounting of abundances over 9 decades in branching fraction [17] with $T_{\rm fo} = 156$ MeV. For reference, the exact observed value $\Omega_{DM}/\Omega_b = 5.3$ is obtained for $T_{\rm eff} = 156$ MeV with $m_S = 1860$ MeV, while for $m_S = 2m_p$, $T_{\rm eff} = 150$ MeV.

One might be tempted to take $T_{\rm fo} = 156$ MeV from relativistic heavy ion collisions and infer m_S from the observed value of Ω_{DM}/Ω_b. However that would not be correct because there are $\mathcal{O}(1)$ uncertainties inherent in the analysis. Most importantly, the turn-on of confinement and chiral symmetry breaking as the Universe cools is almost static and the medium is almost homogeneous, whereas in a heavy ion collision the plasma expands into the vacuum on a short timescale so that $T_{\rm eff}$ can be somewhat different from $T_{\rm fo}$ inferred from fitting heavy ion data [17]. Furthermore, we ignored possible contributions of resonances to particle abundances on account of the long timescale of the Early Universe process, whereas their inclusion improves the fit for Heavy Ion Collisions [17].
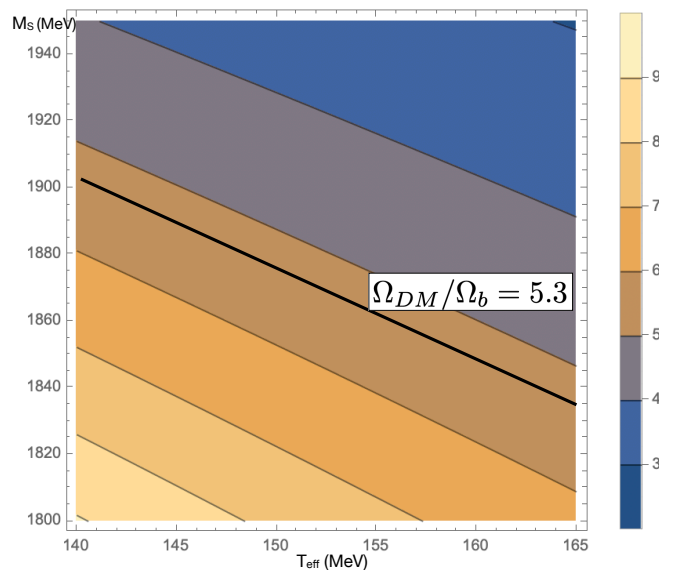

FIG. 2: Ω_{DM}/Ω_b versus m_S (in MeV, vertical axis) and the effective freezeout temperature (in MeV, horizontal axis). The predicted value ranges from 3 (blue) to 8 (light tan); the measured value 5.3 ± 0.1 is indicated by the black line.

We also used $T = 0$ masses in vacuum to estimate κ_s via Eq. (4), whereas hadron masses in a nuclear medium are known from experiment and lattice QCD [18] to differ by $\approx 10\%$ or more from their $T = 0$ values across this temperature range. If a sexaquark would be discovered so that m_S is fixed, the 2% precision with which Ω_{DM}/Ω_b is known will give insight into how QCD condensates and the energy difference of sexaquark-like and hyperon-like states evolve with temperature.

Implicit in the above discussion, is that the value of Ω_{DM}/Ω_b established in the hadronization transition persists to the recombination epoch where it is measured [1]. For sexaquark DM, non-destruction requires the cross section for reactions such as $\pi S \to \Sigma\Lambda$, $KS \to p\Lambda$ and $\Lambda\Lambda \to S\pi\pi$ to be small. This is consistent with the transition amplitude $\tilde{g}$ between an S and two baryons being suppressed, as discussed in the next section.

C. Durability of the S in the hadronic phase

If breakup processes such as $\pi S \leftrightarrow \Sigma\Lambda$, $KS \leftrightarrow p\Lambda$ and $\Lambda\Lambda \leftrightarrow S\pi\pi$ had a typical hadronic rate, these rates would be fast compared to the Hubble expansion rate at the temperatures of interest, $T \sim 150$ MeV. In that case, the S would quickly come into chemical equilibrium with baryons and the chemical potentials would satisfy $\mu_S = 2\mu_b$. However $\mu_S = 2\mu_b$ at $T \sim 150$ MeV, along with $m_S \approx 2m_p$, implies $\lesssim 10^{-7}$ of the baryon number is carried by S's, so an initial SDM excess comparable to the baryon excess would quickly disappear.

Thus we need to estimate the breakup rate of S's. We use lowest order meson-baryon effective field theory extended to

include the sexaquark and SBB' vertices, and elaborate the discussion in [4]. The Lagrangian of the low energy effective field theory describing the interactions between the flavor-singlet S and flavor-octet baryons can be written

$$\mathcal{L} = \frac{\tilde{g}}{\sqrt{40}} \overline{\psi_B} \gamma_5 \psi_{B'}^c S + g_{SSV} S^\dagger \partial_\mu S V^\mu + h.c. \quad (5)$$

where V^μ is shorthand for the flavor-singlet linear combination of ω, ϕ vector meson fields. The second term governs SDM scattering cross sections and we will return to it in later sections. S breakup to baryons is governed by the first term. In Sec. IV we will estimate $\tilde{g}$ theoretically and constrain it from observations. Here, we determine the maximum value of $\tilde{g}$ consistent with SDM surviving in the hot Early Universe.

The color-flavor-spin wavefunction of the totally antisymmetric 6-quark color-flavor-spin singlet state is derived in [19], where it is shown that the quarks in an S have highly entangled wavefunctions such that only a small fraction (1/5) can be decomposed into color singlet pairs of $B = 1$ states. Projecting the S wavefunction in terms of quarks onto that of a pair of color-singlet octet baryons, gives the color-flavor-spin wavefunction-overlap

$$< S \,|\, \Lambda\Lambda > = < S \,|\, \Sigma^0 \Sigma^0 > = - < S \,|\, \Sigma^+ \Sigma^- > \quad (6)$$
$$= - < S \,|\, n\,\Xi^0 > = < S \,|\, p\,\Xi^- > = \frac{1}{\sqrt{40}},$$

motivating the $1/\sqrt{40}$ in the denominator of Eq. (5) so that $\tilde{g}$ is the dynamical transition amplitude $< B\,B' |\mathcal{H}_{\text{QCD}}| S >$ between quarks in the S and those in spatially separated 3-quark states.

The breakup processes with the highest rates are $\pi^\pm S \to \Sigma^\pm \Lambda$ and $K^+ S \to p\Lambda$ with amplitudes

$$\mathcal{M}_{\pi^\pm S \to \Sigma^\pm \Lambda} \approx \frac{f\tilde{g}}{\sqrt{120}} (1-\alpha) m_\Lambda m_\Sigma v_{\text{rel}} \left(\frac{1}{m_\Lambda^2} - \frac{1}{m_\Sigma^2} \right);$$
$$(7)$$
$$\mathcal{M}_{K^+ S \to p\Lambda} \approx \frac{f\tilde{g}}{\sqrt{120}} m_\Lambda m_p v_{\text{rel}} \left(-\frac{(1+2\alpha)}{m_\Lambda^2} - \frac{(4\alpha-1)}{m_\Xi^2} \right).$$

Here $f = 0.952$ and $\alpha = 0.365$ are parameters characterizing the meson-baryon couplings, taken from [20] where they are fit to data, and v_{rel} is the relative velocity in the final state. The v_{rel} factor arises because the baryons must have $L = 1$ in order to satisfy parity and angular momentum conservation and Fermi statistics, given that the π/K is a pseudoscalar, the S is an even parity, spin-0 particle, and the intrinsic parity of a pair of baryons is +1.

Performing the thermal average [21] to determine the SDM breakup rate shows that $\Gamma(K^+ S \to p\Lambda) = n_{K^+}(T) < \sigma_{K^+ S \to p\Lambda} v >$ is about two orders of magnitude larger than $\Gamma(\pi^\pm S \to \Sigma^\pm \Lambda)$, and $\Gamma(\Lambda\Lambda \to S\pi\pi)$ considered in [22]. The suppression of $\pi^\pm S \to \Sigma^\pm \Lambda$ results from the cancelation between the contributions of virtual Λ and Σ in (7) due to the opposite sign of $< S \,|\, \Lambda\Lambda >$ relative to $< S \,|\, \Sigma^+ \Sigma^- >$ in Eq. (6), while $\Lambda\Lambda \to S\pi\pi$ is suppressed by 3-body phase space.

The Hubble expansion rate is greater than the dominant breakup rate $\Gamma(K^+ S \to p\Lambda) = n_{K^+}(150\text{MeV}) < \sigma v >$, for $\tilde{g}^2 < 4 \times 10^{-12}$. In the next section we discuss theoretical expectations and experimental constraints on $\tilde{g}$. As will be seen, the condition $\tilde{g} \lesssim 2 \times 10^{-6}$ is well within the expected range. The assertion of [22] that dark matter cannot be dibaryonic, based on assuming a conventional hadronic breakup rate, is therefore not correct. The related but earlier work of [23] also assumes the relic SDM abundance is determined by the conventional thermal freezeout mechanism, leading them to conclude that a dibaryon mass of order 1.2 GeV is required for dibaryonic dark matter. Instead, the mechanism pointed out in [4] and reviewed above, makes essential use of the fact that chemical equilibrium is not assured in the hadronic phase.

IV. SEXAQUARK BREAKUP INTERACTIONS

A. Modeling $\tilde{g}$

The effective hadronic Yukawa coupling for sexaquark breakup, $\tilde{g}$, is

$$\tilde{g} \, \bar{u}_B \gamma_5 v_{B'} \equiv < B\,B' |\mathcal{H}_{\text{QCD}}| S > . \quad (8)$$

We work in the approximation that this transition amplitude is independent of the baryon masses. Actual transitions of physical interest such as S decay require additional factors of $\mathcal{H}_{\text{w}}$, but these weak interactions are perturbative so to good approximation they factorize from the QCD part of the transition.

The QCD transition amplitude between S and two baryons, distilled into the effective field theory parameter $\tilde{g}$ in Eq. (8), describes the process by which each quark moves from an initial position in the S into a final position in one of the baryons, in the field of the other moving quarks, integrated over all possible paths. The hard-core repulsion of baryons at short distances, responsible for the relative incompressibility of nuclear matter, implies a high potential barrier to the transition between the initial separated configuration and final compact configuration. Furthermore, if the spatial extent of the S wavefunction is of order or smaller than the effective radius of the hard core repulsive B-B potential, the overlap of the initial and final spatial wavefunctions is small as well. These are distinct effects, as can be appreciated by recognizing that even if the S were large compared to the hard core radius and had a similar spatial extent to a deuteron (2 fm), the transition can be highly suppressed if the barrier to rearrangement is high, as exemplified by crystalline phase transitions and protein folding.

The evaluation of $\tilde{g}$ entails relativistic, non-perturbative QCD dynamics whose modeling from first principles is far beyond current theoretical reach. When the number of quarks is larger than 3, even calculating static properties like masses and magnetic moments is challenging, even if the quarks are effectively non-relativistic, which is not the present case. Recognizing the large uncertainties, we proceed to estimate $\tilde{g}$ as a product of the wave-function overlap and a tunneling suppression factor.
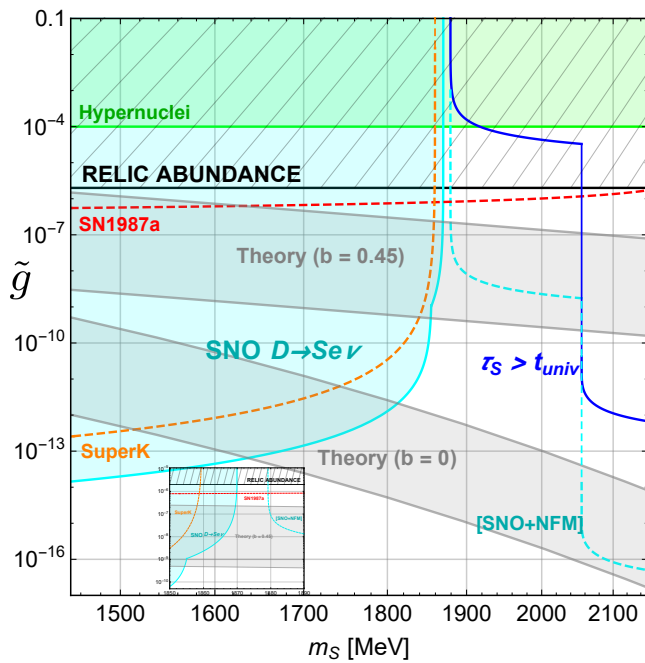
FIG. 3: Predicted and excluded regions for $\tilde{g}$ as a function of m_S; the horizontal black line is the maximum value of $\tilde{g}$ compatible with non-destruction of sexaquark DM in the hot hadronic phase (Sec. III C). The grey bands show the range of theory predictions for $\tilde{g}$, for the extreme values of $0 \leq b < 0.45$ (eq. 1) and taking the hard core radius from fits to scattering data, $r_c = 0.4$ fm (Sec. IV A). The width of the bands reflects the uncertainty range for the tunneling suppression. The bands shift up (down) by a factor $\approx 10^2$ (10^{-3}) for $r_c = 0.3$ (0.5) fm. The green shaded region is excluded by non-production of S in hypernuclear experiments [6]. The cyan shaded region is excluded by our analysis of the stability of deuterons using SNO, reported in Sec. IV B. The dashed orange line is the upper limit from an estimated SuperK background rate [6]. The region above the blue line is excluded in the mass range where decay is kinematically allowed by requiring the S lifetime to be greater than the age of the Universe. The dashed cyan line is a stronger limit that could be obtained from our SNO limits on $S \rightarrow nn$, $n\Lambda$ (Sec. IV C) if the local number density of free SDM particles were $10^{14} \mathrm{cm}^{-3}$ as found in [13], however such a high local number density of free S's can now be excluded by the discussion in Sec. VI. The red line is the limit based on SN1987a cooling following the analysis of [24]; it is shown as dotted because this use of SN1987a has been called into question by [25]. The inset is a blow-up of the 1850-1890 mass range.

The procedure for calculating the wavefunction overlap was developed in [6] where several different nuclear wavefunctions, hard-core radii and model parameters for quark distributions in the Isgur-Karl wavefunction were explored. The value of the most significant parameter – the hard-core radius in the nucleon-nucleon potential, r_c – is uncertain, in part because probing it takes relatively large momentum transfer where a simple potential model description begins to fail. The Hamada-Johnston potential has a hard core of 0.343 fm [26] and the Reid hard core is $r_c = 0.429$ fm [27]; with modern data the hard core radius could possibly be stretched to 0.5

fm, but most likely not more (R. Wiringa, private communication).

The tunneling suppression, e^{-S}, can be estimated as follows. In natural units, the action for a single quark $S_q \sim \Delta E \, t$ with $t \sim$ fm, the time to cross the system (in natural units), and $\Delta E = 100 - 300$ MeV, the QCD scale. Summing over the 6 quarks, the total action for the transition can then be estimated as $S = 3 - 9$, for a tunneling suppression of 0.05 -10^{-4}. This may underestimate the tunneling suppression because lattice gauge calculations show the inter-baryon repulsive potential grows rapidly at short distance, reaching 300 MeV at the shortest distance reported in [28], $r \approx 0.3$ fm, so the typical action per quark may actually be greater than 1.5.

The grey bands in Fig. 3 show $\tilde{g}$ calculated as the product of the tunneling suppression and the spatial overlap, using the consensus value $r_c = 0.4$ fm. The band shifts up (down) by a factor 10^2 (10^{-3}) for $r_c = 0.3$ (0.5) fm. In the lower band, we have taken the radius of the S, which enters the calculation through the Isgur-Karl spatial wavefunction, to be its Compton wavelength. This is motivated because the S does not couple to pions or other light particles and therefore is not spread out by a pion cloud, unlike baryons which couple to pions having Compton wavelength > 1 fm. To show the extreme alternative, in which the S is as strongly coupled to the mediator as the nucleon is to the pion, the upper grey band is calculated with $b = 0.45$. In principle, determination of the Yukawa parameter α_{SN} discussed in the next section would enable the range of b to be narrowed. For further details and plots showing sensitivity to secondary parameters, see [6, 29].

We note that two calculations in the literature did not take proper account of the hard core radius, effectively causing them to overestimate $\tilde{g}$. Ref. [23] follows the analysis of [6] but uses a wavefunction fit to large distance data which does not incorporate hard-core-sensitive information, thus the overlap derived in [23] is much larger and not realistic. Ref. [24] ignores the short distance repulsion altogether and hence greatly overestimates the impact of sexaquarks on the cooling rate of SN1987a.

Although the estimated range for $\tilde{g}$ presented here has large uncertainties, it is far below the $\approx 2 \times 10^{-6}$ value shown by the black line in Fig. 3, where sexaquark breakup would decrease the DM to baryon ratio established in the QGP-hadronization transition. Therefore the prediction $\Omega_{DM}/\Omega_b \approx 5$ of the previous section is a robust prediction of SDM, and its agreement with the observed $\Omega_{DM}/\Omega_b = 5.3 \pm 0.1$ is a significant point in favor of the SDM scenario.

In the next subsections we consider direct experimental constraints on $\tilde{g}$.

B. Experimental constraints on nuclear decay into sexaquark

For $m_D - m_e < m_S < m_D + m_e$, the S and all nuclei are absolutely stable. In this range, the only constraint on the sexaquark breakup or formation vertex $\tilde{g}$ comes from the observed lifetimes of double-Lambda hypernuclei [30–33]. The excluded region from hypernuclei is shown as the green region in Fig. 3.

If $m_S < m_D - m_e = 1876.12$ MeV, deuterium can decay via $D \to S e^+ \nu_e$. The quark-level decay diagrams contain two $u \to s + W^+$ vertices, with one W^+ emitted and another being absorbed, $W^+ d \to u$, for a net quark level transition $ud \to ssW^+$ with amplitude $\sim G_F^2 \sin^2\theta_C \cos\theta_C$. Since we cannot perform a detailed quark-level analysis we capture the essential features of the 3-body phase space by taking the energy dependence to be that of neutron beta decay; inserting the factors from the amplitude and setting $\cos\theta_C$ to 1:

$$\frac{d\Gamma}{dE_e} = \frac{\tilde{g}^2 \, G_F^4 \sin^4\theta_C \, P^6}{120\pi^3 m_D m_S} \sqrt{E_e^2 - m_e^2} E_e (m_D - m_S - E_e)^2. \tag{9}$$

The P^6 factor would emerge from an integration of the quark amplitude over the Bethe-Salpeter wavefunctions of nucleons and S, if those were known and included in the treatment. For our numerical estimates we take $P = 100$ MeV unless otherwise stated, characteristic of the QCD scale. Clearly this is a major source of uncertainty given the high power of P involved. The total decay rate is obtained by integrating Eq. (9) from m_e to $m_D - m_S$.

The SNO detector contains 1000 tons of heavy water. The positrons produced in $D \to Se\nu$ would be detected via their Cherenkov light if the positron's energy is above the SNO 5.5 MeV threshold [34]. (SNO was built to detect electrons produced by solar neutrinos, $\nu_e + D \to 2p + e^-$, but positrons are functionally equivalent to electrons because the spectrum of Cherenkov radiation is only sensitive to charge-squared.) In 391.432 days, SNO has observed $N_{\rm obs} \approx 2465$ $e^\pm$ events with kinetic energies in the 5-20 MeV range, and none above. Let $f(E_{\rm th})$ be the fraction of the spectrum (Eq. 9) above some specified electron total energy threshold $E_{\rm th}$. We obtain limits on Γ and $\tilde{g}$ by requiring (suppressing the dependence of γ and f on m_S):

$$\begin{cases} (f(5.5) - f(20)) \times N_0(1 - e^{-\Gamma t}) < N_{\rm obs}, \\ f(20) \times N_0(1 - e^{-\Gamma t}) < 2.44, \end{cases} \tag{10}$$

whichever is stronger. The 2.44 in the second equation is the 90% CL upper limit when no events are seen; given the large value of $N_{\rm obs}$ and uncertainties in the analysis, we do not correspondingly adjust $N_{\rm obs}$.

The analysis outlined above using SNO data and taking $P = 100$ MeV, gives the cyan exclusion region in Fig. 3. As a result of the uncertainties in calculating the weak-decay amplitude in terms of $\tilde{g}$, the boundary curve should be regarded as a best-estimate indication of the limit on $\tilde{g}(P/100\,{\rm MeV})^3$. Not surprisingly, the limit on $\tilde{g}$ becomes dramatically stronger as m_S drops and phase space for D decay opens up. Due to the wide range of uncertainty in the theory predictions, inverting the bound from D lifetime to get a lower bound on m_S is not very meaningful – especially keeping in mind that $r_c > 0.4\,$fm is not excluded. Nonetheless, one is tempted to deduce provisionally at least, that $m_S < 1800\,$MeV is disfavored even without invoking theoretical prejudices against low masses.

C. Constraints on $\tilde{g}$ from sexaquark lifetime

If $m_S > m_D - m_e$, the sexaquark is not absolutely stable and can decay via $S \to D e^- \bar{\nu}$. Since three-body decay is strongly suppressed near threshold, a more powerful constraint for most of the mass range comes from $S \to nn$, or $S \to \Lambda n$ when that is kinematically allowed. The analysis is straightforward, proceeding along the lines in the previous subsection but simpler due to the 2-body phase space. The pink line in Fig. 3 comes from the constraint that S is longer-lived than the age of the universe. A stronger limit is surely possible, since if $\tau_{\rm DM} = \tau_{\rm Univ}$, 37% of the DM at recombination would have converted to baryons by $z = 0$ with potentially observable implications, but there are other stronger constraints in much of this mass range anyway. (Decaying DM in scenarios with stronger effects than here have been discussed by [35, 36].) For $m_S > m_n + m_\Lambda$ about 8% of the decaying DM mass is converted to radiation (the ultimate γ, e and ν decay products from Λ decay), also having potentially interesting cosmological effects that we do not pursue here.

The cyan dashed line is the stronger limit which would follow from SNOlab limits on neutron production, if the ambient density of S's in the SNOlab detector were $n_S = 10^{14} {\rm cm}^{-3}$. This scenario is motivated by the Neufeld et al. [13] calculation of the DM atmosphere of Earth as a function of DM mass and interaction cross section, in the approximation that the Earth's atmosphere and geophysics have been constant over its lifetime. With this caveat, the predicted abundance of DM near the Earth's surface reaches $10^{14} {\rm cm}^{-3}$ for DM mass in the sexaquark range. If such a DM atmosphere consists of free sexaquarks able to decay, the resulting limits on the S decay lifetime are shown by the cyan-dashed line in Fig. 3.

The bound is calculated as follows. Phase III of the SNO experiment was equipped with an array of ^{3}He neutron counters [34] and therefore, neutrons produced from $S \to nn$ could be detected. We require

$$n_S V \times (1 - e^{-\Gamma t}) \times 2 \times \epsilon < N_{\rm obs}, \tag{11}$$

where $V = 904.78$ m^3 is the volume of the tank, $\epsilon = 0.182$ is the detector efficiency, and $N_{\rm obs} \approx 7000$ is the observed number of neutron events during $t = 385.17$ days. Taking $n_S \sim 10^{14}$ cm^{-3} to be the ambient density of SDM in SNO, Eqn. (11) implies $\tau \gtrsim 4.96 \times 10^{18}$ yr at 90% confidence level.

However this limit on $\tilde{g}$ is evaded or weakened if the ambient DM is hybridized with nuclei in the Earth and kinematically unable to decay (Sec. VIII B), if the DM-nucleon interaction is repulsive so dewar exclusions exclude it (Sec. VI B), or if the DM atmosphere calculated in Ref. [13] is overestimated, e.g., due to significant disturbances in the temperature profile of the upper atmosphere producing periods of increased for DM evaporation.

D. Cooling of SN1987a

Ref. [24] argued against a deeply bound dibaryon such as the sexaquark, on the grounds that the reaction $\Lambda\Lambda \to S\gamma$,
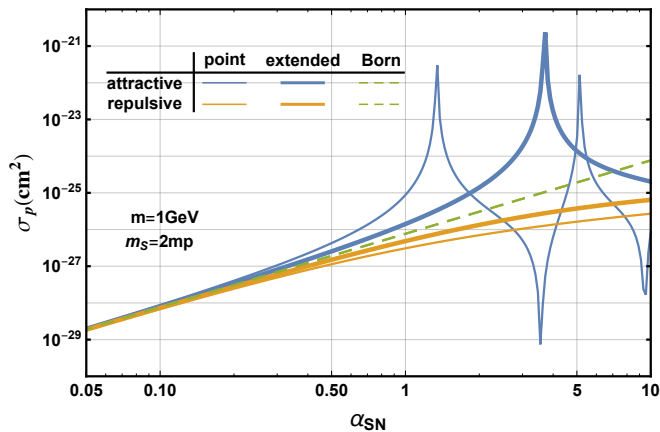
FIG. 4: The S-proton cross section σ_1 as a function of α_{SN}. Born approximation becomes inaccurate at the 30% level for $\alpha > 0.25$; for nuclei Born approximation fails at still smaller α.

would cause SN1987a to cool too fast to account for the neutrinos arriving over 10 s. The general use of this cooling argument has been called into question in Ref. [25], proposing another mechanism for producing last neutrinos that is independent of the proto-NS cooling. Nonetheless, it is interesting to determine what bounds on $\tilde{g}$ could be derived under the assumption of a 10s cooling time. We follow the analysis of [24] but invert it to find a limit on $\tilde{g}$; this bound is shown as the red dashed line in Fig. 3. The limit on $\tilde{g}$ needed to satisfy a 10s cooling time is clearly compatible with the predicted range of $\tilde{g}$. The discrepancy between this result and the conclusion of [24] that an S in this mass range is ruled out by SN1987a, is due to their neglecting the hard-core repulsion between baryons that strongly inhibits production of S's.

V. SEXAQUARK SCATTERING INTERACTIONS

The low-energy interaction between sexaquarks and baryons is mediated by exchange of massive QCD mesonic states, which are constrained by low-energy nucleon and nuclear interactions. Thus the interactions of SDM with baryons are not arbitrarily adjustable as is often possible in beyond-the-standard model DM scenarios. In the non-relativistic limit, which is applicable for all the processes we are considering, the elastic scattering of DM by baryons can be described by a Yukawa potential

$$V(r) = -\frac{\alpha}{r} e^{-mr} \; , \qquad (12)$$

where the minus sign is for convenience so that $\alpha > 0$ corresponds to an attractive force and $\alpha < 0$ repulsive. The attractive case has a richer phenomenology, as discussed below. Because the discussion here is more general than for S's, we designate the mediator as m and drop the subscript from α_{SN} when not needed for clarity.

As already noted, since the S is a flavor-singlet, the lightest meson giving a significant contribution is the flavor-singlet combination of $\omega - \phi$ mesons designated V. (The scalar f_0, an extended di-meson resonance, is expected be very poorly coupled to the compact S.) Taking the mixing angle from [37] we have

$$|V> = 0.8 |\omega> - 0.6 |\phi> \; , \qquad (13)$$

where $m_\omega = 782$ MeV and $m_\phi = 1020$ MeV [5]. The coupling strength α_{SN}

$$\alpha_{SN} \equiv g_{SSV} \, g_{NNV} / 4\pi \qquad (14)$$

may be as large as $\mathcal{O}(1)$, as is typical for strong interaction processes, or it may be much smaller depending on g_{SSV}, the coupling of V to S appearing in the low energy effective Lagrangian, Eq. (5).

From [37], $g_{NNV}/\sqrt{4\pi} = 2.5$, but we stress that modern analyses of low energy baryon-baryon scattering such as [37, 38] are much more sophisticated than a simple one-meson-exchange treatment and include many exchanges and other effects. Thus while the parameters in those analyses have small error bars, used out of the context of those full analyses a parameter such as $g_{NNV}/\sqrt{4\pi} = 2.5$ should be considered to have $\mathcal{O}(1)$ uncertainties and just considered as a guide for our problem. An estimate of the minimum coupling strength range of g_{SSV} might be to rescale $g_{NNV}/\sqrt{4\pi} = 2.5$ by the square root of the ratio of the size of the S and V (taking the N and V to be fully overlapping and strongly coupled). With r_S as small as 0.1 fm, and $r_V \approx 1$ fm, this would suggest g_{SSV} a factor 30 smaller than g_{NNV}. Adding a margin of uncertainty in both directions, we focus our attention on the domain $0.001 < \alpha_{SN} < 10$.

An exact analytic solution for the Yukawa potential scattering problem does not exist and Born approximation does not apply for the parameter space we are interested in so that a full numerical solution is necessary. Furthermore, since nuclei are extended, we need to solve the Schroedinger problem for the extended potential obtained by smearing the Yukawa over a hard sphere of radius $R_A \approx R_0 A^{1/3}$ fm. We took $R_0 = 1.0$ for the calculations presented in this paper, but models in the literature have values up to 1.25. Sensitivity of our results to the value of R_0 will be reported in [39], where details of our calculational methods are given. We rely heavily on techniques from [40]. Note that for a given model of the nuclear wave function the constraints on α_{SN} derived in this and following sections can generally be determined to higher precision than 1 significant figure, but on account of our simplistic approximation that the nucleus is a hard sphere of radius $A^{1/3}$ fm, reporting higher precision would be misleading.

Figures 4, 5 and 6 show the first crucial result: the inapplicability of the Born approximation over a large portion of parameter space. Fig. 4 shows how the DM-proton cross section, σ_1, depends on α for extended and point sources and attractive and repulsive interactions. (We abbreviate $\sigma_{SA} \to \sigma_A$.) For $\alpha \gtrsim 0.1$ the Born approximation is inaccurate, with the true cross section being lower than Born approximation for the repulsive case. For an attractive interaction the true cross section is up to a factor 10^5 higher and 10^4 lower than Born, as α ranges from 1 to 5 in the pure Yukawa case; for an

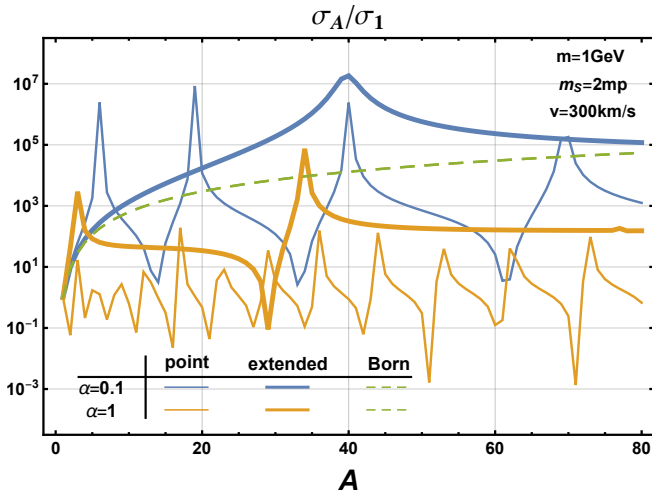FIG. 5: σ_A/σ_1 versus A for $v = 300$ km/s and $\alpha_{SN} = 0.1$ and
1.0 (blue, yellow), for an attractive Yukawa interaction and point
and extended nuclei (thin and thick curves, respectively); the Born
approximation ratio is shown in green-dashed. Born approximation
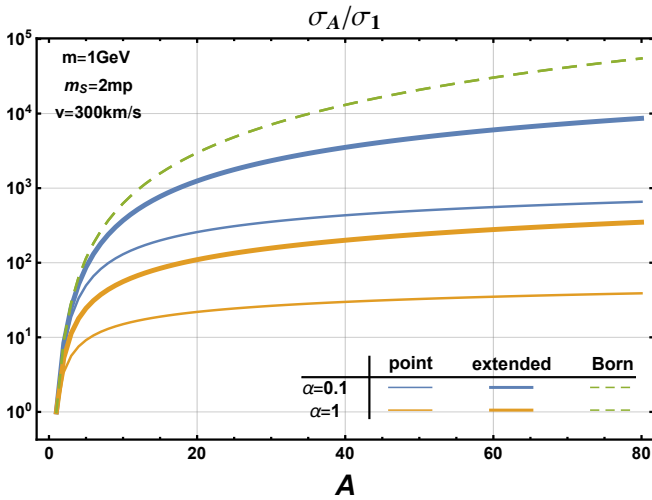fails badly for all cases.

FIG. 6: As in Fig. 5 but for a repulsive interaction. Born approxima-
tion overestimates σ_A/σ_1 in all cases, by a factor ≈ 40 for Si with
$\alpha_{SN} = 1$ and realistic nuclear spatial distribution.

extended source such extreme deviations are pushed to larger
α.

Figures 5 and 6 show how the cross sections scale *relative
to Born approximation* as a function of A. Born approxima-
tion implies the following scaling of the nuclear cross section

$$\sigma_A^{\text{Born}} = \sigma_p^{\text{Born}} \left(\frac{\mu_A}{\mu_p}\right)^2 A^2 , \qquad (15)$$

where μ_A is the reduced mass of the SA system. This scaling
fails badly even for $\alpha = 0.1$, for all cases: for both repulsive
and attractive interactions and for both extended and point-
like sources. In the repulsive case, the true cross section is
significantly lower than predicted by the Born approximation

and the discrepancy increases with A. There is no such simple
relation in the attractive case, although at small α_{SN} the true
cross section is larger for the realistic extended case, while for
large α_{SN} the situation is more complicated.

The peaks and valleys in cross section for the attractive
case can be understood as follows, focussing on the point-
like (exact Yukawa) case where the discussion is simple. The
Schroedinger equation for the Yukawa potential can be put
into dimensionless form such that σm^2 is a function only of
the dimensionless parameters (in natural units, with $c = 1$)
[41]:

$$a \equiv \frac{v}{2\alpha} , \quad b \equiv \frac{2\mu\alpha}{m} , \quad x \equiv 2\mu\alpha r , \quad \tilde{V}(x) = -\frac{1}{x}e^{-\frac{x}{b}} , \qquad (16)$$

where as before μ is the DM-nucleus reduced mass and m is
the mediator mass. Evidently, b sets the range of the potential.
At low energy S-wave scattering ($l = 0$) is dominant so the
cross section is

$$\sigma_{\text{S-wave}} = \frac{4\pi}{a^2 b^2 m^2} \sin^2(\delta_0) . \qquad (17)$$

When the S-wave phase shift $\delta_0 \to \frac{\pi}{2}$, the cross section is
on resonance and reaches its maximum value. The position
of the peaks are in one-to-one correspondence with the zero
energy bound states of the Yukawa potential. When b is small
the potential is too narrow/weak to accommodate any bound
states. As b increases, the potential becomes wider/stronger,
up to the point where a bound state with $E_0 \to 0^-$ appears,
at which value particle scattering has maximum cross section.
As b continues to increase, the ground state binding energy
gets more and more negative, up to some point where an-
other bound state with $E_1 \to 0^-$ emerges and there is an-
other peak in the scattering cross section. The position of
these zero energy bound states are easily calculated to be at
$b = 1.68, 6.45, 14.34...$, which is exactly where the peaks in
the cross section are located. The physical implications of the
bounds states that exist when the potential is attractive is dis-
cussed in Sec. VIII below.

On the other hand when $\delta_0 \to n\pi$ the S-wave cross section
vanishes, which is an anti-resonance and corresponds to the
dips in the cross section. The small cross sections at the anti-
resonances lead to gaps in the exclusion limits, as we shall see
below. The anti-resonances are not associated with any bound
state behavior; they occur at $b = 4.52, 11.84, ...$

The existence of resonance and anti-resonance scattering is
associated with non-trivial velocity dependence of the cross-
section, as shown in Fig. 7. On resonance, $\sigma \sim v^{-2}$ at
small velocity for a pure Yukawa, leading to the enhanced
cross-section. For generic values of b the cross section is
roughly constant for small b, but as the anti-resonance is ap-
proached ($b = 4.52$ for point-like source), the cross section
is diminished at small velocities. At large velocities, for all b,
$\sigma \sim v^{-4}$ and the scattering is Coulomb-like. The transition to
this regime occurs for $a > a_{\text{crit}}(b)$. When the source of the
Yukawa is smeared over a nucleus, the behavior is different
but still non-trivial. Fig. 8 shows the behavior for repulsive
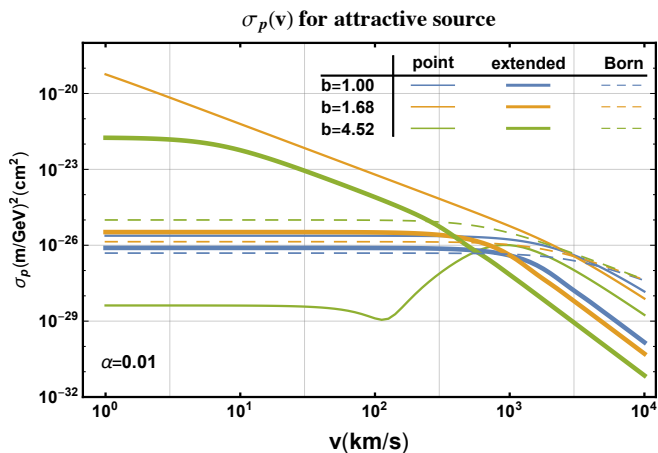interactions, where there is no resonance or anti-resonance.

FIG. 7: Velocity dependence of σ_1 for an attractive interaction with $\alpha = 0.01$, for 3 values of b. $b = 1.68$ (ochre) is on resonance and $b = 4.52$ (green) is on anti-resonance for the point-like case while the resonance and anti-resonance occur for different b's for an extended source.
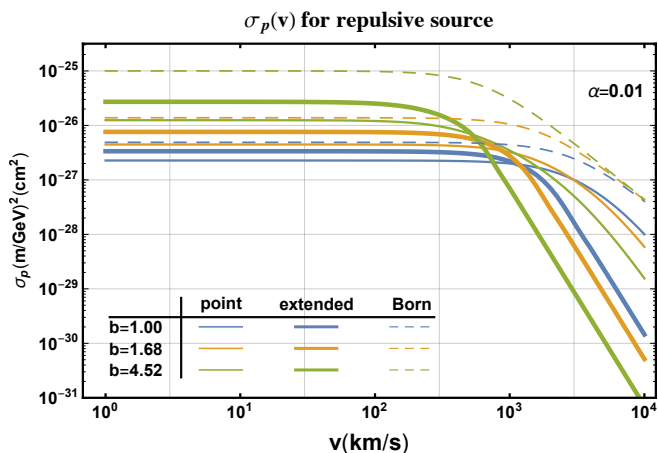

FIG. 8: As in Fig. 7, for repulsive interaction. Note the different vertical scale.

VI. DIRECT DETECTION AND COSMOLOGICAL LIMITS

In view of the highly non-perturbative behavior seen in Figs. 4 - 6, we must re-examine the existing limits on DM-nucleon interactions. The limits on spin-independent cross sections are almost universally reported as bounds on the DM-nucleon cross section. However in almost all cases, what has actually been done is to use Born approximation and the A-scaling it implies to convert experimental limits on σ_A to the reported limit on σ_1. The cross section is usually assumed to be independent of v, or in some analyses various power-law dependences are explored.

Here, we report excluded regions in the α_{SN}-m_S (more generally α-m_{DM}) plane, which is the most fundamental information, rather than reporting limits on σ_{DMp}. For a given α and DM particle velocity and mass, we use the correct value

of the cross section from high-resolution tabulated numerical solutions to the Schroedinger equation. This naturally incorporates the actual velocity dependence which as seen above is not in general a simple power-law at all velocities. We generally report limits taking $m = 1$ GeV.

A. Correcting the XQC limits

The X-ray Quantum Calorimeter [42] was an experiment to measure the diffuse X-ray background using microcalorimeters onboard a sounding rocket at about 100 km altitude in the atmosphere. The results can also be used to put limits on the DM-nucleon cross section, and extensive studies have be performed [43–46]. The analyses prior to [46] all assumed that the entire recoil energy of the Si nucleus ($\sim$ keV for DM mass of 2 GeV) is converted to phonons in the XQC calorimeter. However as pointed out in [46], at these low energies below ionization threshold, the recoiling Si atom moves as a whole and produces a cascade of dislocated atoms – very low energy (few eV) lattice defects called Frenkel pairs consisting of a hole in the lattice and an interstitial Si atom [47–54]. Similar effects can be expected in sapphire and other materials used for micro-calorimeter detectors [55]. So rather than being thermalized, the energy deposited by the DM collision may be stored in Frenkel pairs. Limiting the production of such point defects (vacancies and interstitial atoms) during the process of crystal growth, is an important commercial in the semi-conductor industry. For a review see [56]. A typical concentration of defects is 10^{15} cm^{-3}; compared to this, the increment in defects during the course of the 100 s XQC mission is negligible, as we now show.

The Galactic DM abundance in the solar neighborhood is ≈ 0.3 GeV cm^{-3}. Taking $m_S = 2m_p$ and DM velocity ≈ 300 km/s, the flux of SDM is $\approx 10^6$ cm^{-2}s^{-1}. The fraction of the DM kinetic energy deposited per scattering is

$$f_{\mathrm{KE}} = 2(1 - \cos\theta)\frac{m_{\mathrm{DM}}m_{\mathrm{A}}}{(m_{\mathrm{DM}} + m_{\mathrm{A}})^2}, \qquad (18)$$

where θ is the CM scattering angle. For $m_{\mathrm{A}} >> m_{\mathrm{DM}}$, appropriate for SDM and detectors like XQC, and noting that the scattering is isotropic in the CM, the average kinetic energy deposited in the initial collision is ≈ 100 eV, thereby producing $\lesssim 100$ point defects. Even if every DM particle scattered once (vastly more than consistent with expectations and other constraints), the increment in the density of defects in a 3 mm thick Si detector in the 100 s flight would be $\lesssim 10^{11}$ cm^{-3} – more than 4 orders of magnitude less than the initial density of defects and hence not noticeable at all. Likewise the impact of DM on the abundance of point defects at sea-level is insignificant: if the scattering cross section is large, the ambient DM at sea level carries little energy and a scattering produces few or no defects, whereas if the cross section is small, DM-scattering is a minor contributor to the point-defect population. Perhaps some detection strategy could make use of this process, however.

Due to the likelihood that recoiling atoms deposit their energy in creation of Frenkel pairs rather than in thermal excita-

tions of the material, until the thermalization efficiency of detectors such as XQC, DAMIC and CRESST is measured with neutron scattering, limits from those experiments can only be discussed in terms of their potential sensitivity, not as actual exclusion limits.

The blue shaded region of Fig. 9 shows our exclusion region in the $\{\alpha, m_{\mathrm{DM}}\}$ plane from XQC data, for a mediator mass of 1 GeV. We adopt the fiducial thermalization efficiency $\epsilon_{\mathrm{th}} = 0.01$; this is at best an indicative, round-number value motivated by a Frenkel-pair cascade analysis [46]. We follow the XQC analysis of [46] but solve the Schroedinger equation for the extended Si nucleus to obtain the cross section, rather than using the A scaling from Born approximation and the Helm form factor. (It should be noted that the Helm-form factor gives a poor approximation to the impact of an extended source, so replacing the Born approximation is not enough; see [39] for details.) Future analyses of direct detection experiments aiming to detect DM under an overburden will also need to take into account the possibility of DM capturing on a nucleus en route to the detector, as discussed in Sec. VIII B below.

B. Limits from dewar experiments

It was pointed out by Neufeld et al. [13] that if the DM cross section on nuclei in the Earth's crust and/or atmosphere exceeds $\approx 10^{-28.5}\,\mathrm{cm}^2$, a DM atmosphere forms around the Earth; the density distribution of this atmosphere was characterized under the assumption that the atmosphere of the Earth has been reasonably steady over its lifetime. The density of DM particles near the surface of the Earth reaches $\approx 10^{14}\,\mathrm{cm}^{-3}$ for $m_{\mathrm{DM}} \approx 2m_p$. The presence of such a high density of DM, if it is free rather than bound to nuclei, produces detectable effects that Ref. [13] used to place limits on DM interactions with various materials. The limits included heating of liquid He and other cryogens in dewars, HST orbital drag, and modification to the thermal conductivity of the Earth. Stronger upper limits on σ_A were obtained for many more individual A values by dedicated dewar experiments in which samples of different A were placed in a dewar of liquid nitrogen and the evaporative mass loss after a time interval was measured [58].

Interpreting the limits on σ_A for the ensemble of A's is challenging due to the non-trivial dependence of σ_A on α as discussed in the previous section (Sec. V). Basically it entails stepping through the full parameter space, determining at each point in parameter space the local number density based on the DM scattering cross section with air or crust including capture and evaporation from Ref. [13], then calculating the corresponding heating due to DM collisions for pellets of the given A. (We thank D. Neufeld for providing necessary input data.) Details of how this was done are presented in [39].

The green-bounded region in Fig. 9 is the nominal resultant exclusion region for an attractive DM-nucleon interaction. The boundary in the repulsive case is similar but smoother; a plot for the repulsive case can be found in [39]. To get an estimate of the uncertainty in the excluded region from the
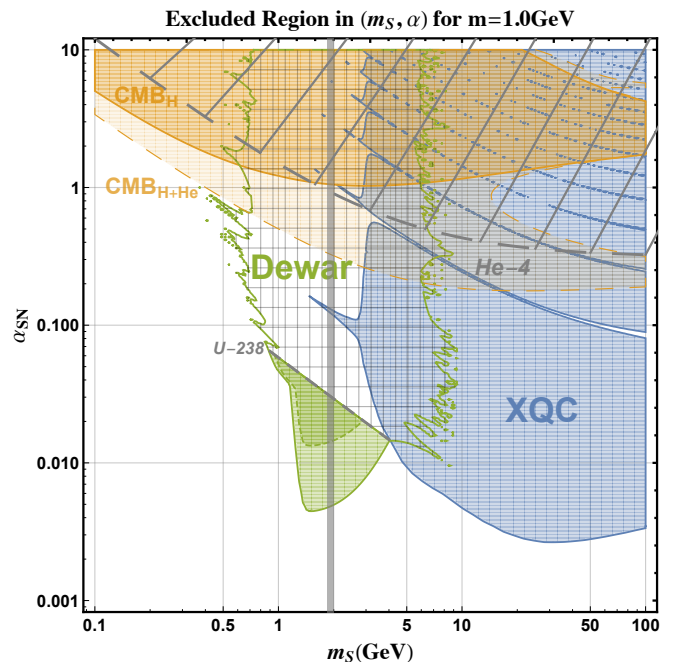

Excluded Region in (m_S, α) for m=1.0GeV

FIG. 9: Excluded regions in the α_{SN}-m_S plane from XQC (blue), CMB (tan) [57] and dewar experiments (green&checkerboard), for an attractive SN interaction. (If the DM-nucleon interaction is repulsive, the plot is similar except that the XQC and dewar boundaries are smoother and the dewar limits exclude the entire green-bounded region; see [39].) The thin vertical grey band marks the range $m_S = 1860 - 1890$ MeV. The diagonal-hatched region above the upper grey-dashed line is excluded by the requirement that primordial ^{4}He not hybridize with DM. Within the checkerboard region the dewar limits are inapplicable when the interaction is attractive, because DM would hybridize with nuclei in Earth's crust. The darker green region with dashed boundary shows the dewar exclusion in case the local DM density is a factor-10 lower than calculated by [13], to give an indication of the sensitivity. The light tan region bounded by dashed lines is a potential exclusion region estimated from the CMB analysis of [57], approximately taking into account "resonant" DM-^{4}He scattering.

dewar experiments and obtain a more conservative limit from the dewar experiments, we can take a factor-10 lower SDM atmosphere than estimated in Ref. [13]. Such a reduction might arise from a lower Galactic DM flux or possible disruptions in the accumulation of a DM atmosphere. This reduces the size of the excluded region below the U-238 line as indicated by the darker green region; for $m_S = 2m_p$ the limit on α_{SN} becomes 0.015.

Note, however, that when the interaction is attractive and $\alpha_{SN} \gtrsim 0.04$, the dewar exclusion shown Fig. 9 is evaded. In that case, SDM in the Earth binds to nuclei as discussed in Sec. VIII B. DM particles bound to nuclei cannot freely penetrate through the walls of the dewar and heat the material, so the dewar limits on DM interactions do not apply; all other limits of [13] are evaded as well. The cross-hatched region shows the part of the XQC exclusion region that is eliminated for this reason.

C. Limits on DM-baryon interactions from structure formation

The cross-hatched region above the upper grey line is excluded for an attractive interaction because primordial He would hybridize with S's shortly after being produced. The region labeled CMB follows from the limits on σ_{DM-p} obtained in Ref. [57] from the damping of structure formation that results from DM-p interactions, translated to α, m_{DM} space taking the proton to be a hard sphere of radius 1.0 fm. The lighter region bounded by dashed lines and labeled CMB_{H+He} is derived from limits of [57], but instead of assuming a fixed ratio σ_{SHe}/σ_{Sp} based on Born approximation (their Eq. (14)) and a coupling proportional to charge, we used the actual ratio determined by each α, m_{DM} pair and the Schroedinger equation. For α_{SN} such that He scattering is in the "resonance" region, He completely dominates H in its drag on DM. But recombination of He occurs at higher z than for protons, so the rough estimation employed here probably exaggerates the limit. We present it here because this is an interesting region of parameter space in connection with exotic isotopes and deserves a dedicated cosmological study along the lines of [57].

The recent limits from [59] are not directly applicable to SDM because non-gravitational DM-baryon interactions modify the structure of cores of dwarf galaxies, potentially modifying the mapping from as-observed dwarf properties to linear-regime structure used in [59]; another issue which has not yet been examined by the community is the extent to which uncertainties due to the complexities of baryonic physics have a significant impact on the analysis of [59].

D. Astrophysical Limits

Ref. [60] reports limits on dark matter-ordinary matter cross sections for a number of dark matter scenarios, from bounds on the heating or cooling of the Leo T dwarf galaxy and Milky Way gas clouds due to DM scattering on nucleons and electrons. The strongest limits for DM-nucleon scattering for $m_{DM} \approx 2m_p$ come from the gas clouds, whose limit is included in Fig. 9. It is quite similar to the CMB limit for the $m_{DM} \approx 2m_p$ region of interest for SDM. Given the entirely different uncertainties entering the cosmology and astrophysics analyses, it is useful to have both. The limit from Ref. [60] is similar to the limit from requiring that primordial ^{4}He does not form bound states with SDM, but applicable for either attractive or repulsive interactions.

VII. SELF-INTERACTING DARK MATTER

Spergel and Steinhardt [61] pointed out two decades ago that DM self-interactions of order $\sigma/m_{DM} \sim 1\,\mathrm{cm}^2/\mathrm{g} (= 1.78 \times 10^{-24}\,\mathrm{cm}^2/\mathrm{GeV})$ could explain the observed cores in galaxy centers, whereas cosmological simulations predicted cusps. More realistic treatment of baryonic physics since 2000 alleviates the most severe problems of LCDM, so the call
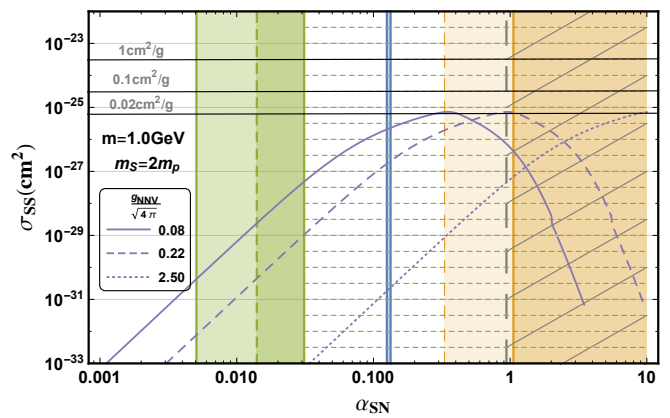

FIG. 10: The SIDM cross section as a function of α_{SN} taking $m_S = 2m_p$ and $m = 1$ GeV, for $g_{NNV}/\sqrt{4\pi} = 2.5, 0.22$ and 0.08, with the key limits from Fig. 9. The green range $0.015 < \alpha_{SN} \lesssim 0.03$ is excluded by dewar limits (less conservatively, 0.005-0.03) while the tan region is excluded by the CMB. The pale tan is the estimated potential exclusion region by extending the CMB analysis to ^{4}He with non-perturbative interactions as discussed in the text. The horizontal black lines mark $\sigma_{SS}/m_{DM} \sim 1$, 0.1 and $0.02\,\mathrm{cm}^2/\mathrm{g}$, suggesting that sexaquark dark matter does not have sufficiently strong self-scattering cross section to have a significant astrophysical impact.

for self-interacting DM (SIDM) is less pressing. However problems with LCDM continue to be identified, e.g., [62], and several authors argue that a much better accounting is obtained of galactic dynamics with self-interactions of order $\sigma/M \approx 1\,\mathrm{cm}^2/\mathrm{g}$. The literature is very large; see [63–65] for examples of recent papers and [66] for a review. For the characteristic SDM mass $m_{DM} = 2m_p$, $\sigma/M \approx 1\,\mathrm{cm}^2/\mathrm{g}$ translates to $\sigma_{SS} = 3.34 \times 10^{-24}\,\mathrm{cm}^2$, at velocities ≈ 100 km/s relevant to the small scale structure of galaxies.

SDM has self-interactions via exchange of whatever produces its interactions with nucleons, identified here as predominantly due to the exchange of the flavor-singlet vector meson denoted here by V (Sec. V). Taking the S interaction to be dominated by V exchange, the self-interaction is repulsive because like charges repel for vector exchange. The Yukawa interaction has the same form as in Eq. 12, with

$$\alpha_{SS} = \left(\frac{\alpha_{SN}}{g_{NNV}/\sqrt{4\pi}}\right)^2 = 0.16 \left(\frac{2.5}{g_{NNV}/\sqrt{4\pi}}\right)^2 \alpha_{SN}^2 ,$$
(19)

where $g_{NNV}/\sqrt{4\pi} = 2.5$ is taken from the Nijmegen Soft Core NSC89 its (Table VI of [37]). Note, however, that although low energy hadron interactions have been modeled in detail, there is a factor-few uncertainty in the estimate (19) because we ignore here the derivative (f) coupling of the V and because the V couplings obtained with the more elaborate ESC19 Extended Soft Core model [38] differ from those from NSC89, especially the f couplings. Although we drop those contributions, they can interfere and cause significant cancelations or enhancements.

Figure 10 shows the SS cross section as a function of α_{SN}, with $m_V = 1$ GeV and several choices for $g_{NNV}/\sqrt{4\pi} =$

2.5, 0.22 and 0.08. Exclusion regions from the previous section if the S-nucleon interaction is attractive are also indicated. The cross-hatched region is excluded by the requirement that sexaquarks do not bind to ^{4}He. The orange region is excluded by our analysis based on the CMB limits on $\sigma_{\mathrm{DM-p}}$ of [57], and the pale-orange region by the estimated extension to ^{4}He discussed in Sec. VI C. The green region is excluded by the [13, 58] dewar limits and the blue region by XQC. The horizontal lines mark $\sigma/m_{\mathrm{DM}} \sim 1$, 0.1, $0.02\,\mathrm{cm}^2/\mathrm{g}$ taking $m_S = 2\,m_p$. One sees from Fig. 10 that the maximum value $\sigma/m_{\mathrm{DM}} \approx 0.02\,\mathrm{cm}^2/\mathrm{g}$, which is lower than usually considered by advocates of SIDM to improve the description of galaxies relative to LCDM. The maximum value may be lower still, depending on α_{SN} and $g_{NNV}/\sqrt{4\pi}$. Given that SDM also interacts with baryons, it is possible that considering both self- and baryonic interactions, SDM can give as successful a description of galaxies as claimed for SIDM, with a lower self-interaction cross-section than needed in pure SIDM.

VIII.   PRODUCTION OF EXOTIC ISOTOPES

DM-nucleus hybridization takes place at a phenomenologically interesting level, if a bound state exists and the relative velocity is sufficiently low for capture to occur, in regions of the Universe with sufficiently high density of both SDM and nuclei of mass $A \geq A_{\mathrm{min}}(\alpha_{SN})$. Fig. 11 shows that the binding energy of a sexaquark to a nucleus of mass A is typically $\approx$ 0.1-10 MeV over the range of α_{SN} large enough to produce binding for $A \lesssim 40$. Therefore most bound states would survive in most astrophysical environments, once produced. In this section we consider two particularly relevant production sites, Big Bang nucleosynthesis and in the Earth.

Avoidance of creation of abundant (and not observed) primordial ^{4}HeS implies $\alpha_{SN} \lesssim 0.7$ as discussed in Sec. VIII A below, which has the further consequence that sexaquark binding only occurs at a significant level with nuclei produced in stars and their explosions and mergers. This means that non-negligible levels of hybrid nuclei is restricted to baryon-dominated environments, so that depletion of free SDM by binding to baryons has only a higher-order impact on the CDM character of SDM.

Denoting the hybrid nucleus-sexaquark state by AS, the dominant capture process is $S + A \rightarrow AS + \gamma$, analogous to the case for neutron capture. The theory of neutron capture is well-developed due to its importance in nucleosynthesis and nuclear physics, c.f., [67]. At intermediate to high incident energy, resonance intermediate states can be excited, but at the low energies relevant here, the most important contribution to the amplitude is due to "direct capture" with the nucleus a passive source of the potential. Because the potential well is shallower in the AS case than for nuclei, given the α_{SN} range of interest, the dominant contribution to the capture cross section is from an initial p-wave scattering state into the (s-wave) bound state with emission of an E1 photon. Derivation of the capture cross section in this case will be presented elsewhere [68].
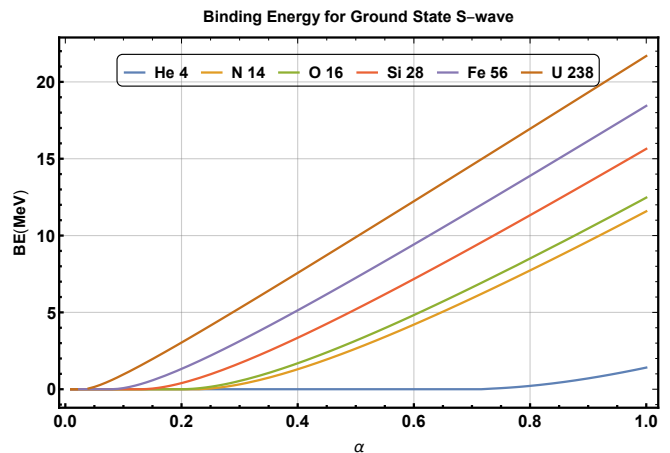

FIG. 11: Binding energy of a sexaquark to selected nuclei as a function of α_{SN}.

A.   Primordial nucleosynthesis

SDM can potentially impact primordial nucleosynthesis in two ways:
1) interference with the standard synthesis process by disruption of intermediate or final nuclei, and/or
2) production of hybridized nuclei, if the interaction is attractive and sufficiently strong to form a bound state.

Our colleague R. Galvez modified the BBN code AlterBBN [69] to allow for SDM-nucleus interactions. He found that even with the DM-nucleus cross section at its unitarity limit, nuclear breakup by SDM scattering ($A + S \rightarrow A_1 + A_2 + S$, e.g., $^7Be + S \rightarrow^3 He +^4 He + S$) is negligible. This stems from the kinematic fact that in the temperature range at which nucleosynthesis occurs, $T \lesssim 80$ keV, $i)$ the available energy in the final state is so small that 3-body phase space suppression is very large and $ii)$ the energy transfer in collisions between nuclei and SDM is too small to overcome the potential barrier to breakup except in the extreme tail of the Boltzmann distribution, even for the least-bound nucleus ^{7}Be.

However as noted in Sec. V, if the S-nucleon interaction is attractive, S forms bound states with nuclei of $A > A_{\mathrm{min}}(\alpha_{SN})$. The minimum nuclear mass to form an A-S bound state increases as the coupling strength α_{SN} decreases. The relationship is shown in Fig. 12. It is very important to stress that all A above some minimum value A_{min} which depends on α_{SN} will form bound states. If nucleus A hybridizes, so do all heavier nuclei, in the approximation of spherical homogeneous nuclei with radii increasing as $\sim A^{1/3}$.

For the α_{SN} range of interest, hybridization occurs at a rate much higher than the expansion rate of the Universe at the BBN epoch ($\tau_{\mathrm{Univ}} \approx 100$ s). Thus hybridized and unhybridized states are in chemical equilibrium. Unless the binding energy is very small, statistical physics favors hybridization so we require α_{SN} to be small enough that no essential primordial nuclei forms a bound state with S. This constrains $\alpha_{SN} \lesssim 0.7 - 0.8$ in the attractive case, to avoid that primor-
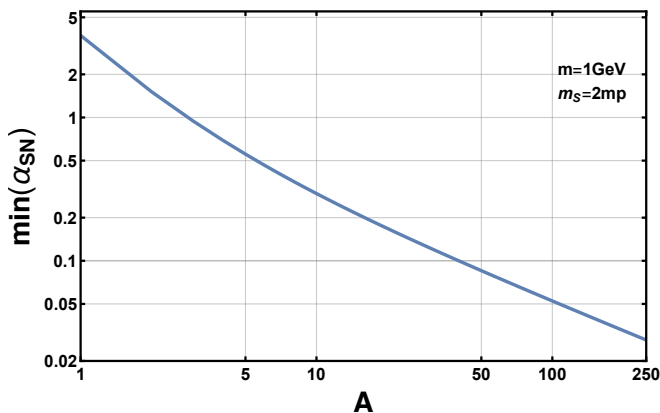
FIG. 12: The minimum α_{SN} such that a bound state AS can form; $\alpha_{SN} \gtrsim 0.7$ is excluded by non-binding of primordial ^{4}He. Mentally inverting axes, the plot also gives $A_{\min}(\alpha_{SN})$, the minimum A which forms bound states for given α_{SN}.

dial He is not in fact HeS with mass ≈ 6 amu. As noted, this condition also insures that no other nucleus having $A \leq 4$ can hybridize.

An enticing scenario for explaining the deficit of primordial ^{7}Li as inferred from the Spite plateau [70–74], would be if ^{7}Be hybridized such that the electron capture production of ^{7}Li or ^{7}LiS was suppressed or forbidden. While this can be contrived [39], it does not solve the problem because then ^{7}BeS should be present at the level expected for ^{7}Li, whereas the upper limit on Be in dwarf stars is much lower [75, 76]. (The isotope shift for 2 amu higher mass is small relative to the widths of the lines used to identify Be or Li, so a hybridized component in the elemental abundance would not be missed. We have not explored whether hybridization of nuclei with $A > 4$ during BBN could diminish production of ^{7}Li and resolve the ^{7}Li puzzle.)

B. Exotic isotope formation in Earth and its atmosphere

Dedicated studies place very stringent limits on the local abundance of exotic isotopes with $\gtrsim 100$ GeV mass splittings relative to the normal nucleus [77–83]. However limits have yet to be developed for mass splitting close to 2 amu, as is relevant for the exotic isotopes formed if SDM hybridizes with nuclei. In this section we take a first look at possible exotic isotope abundances for attractive SDM. Many of the most important nuclei in the Earth have stable isotopes with $A + 2$, with natural abundances generally much larger than expected for SDM hybrids, so dedicated experiments to search for the predicted isotopes will be required for most cases, to discriminate between an $A + 2$ nucleus and an AS bound state.

As shown in [84], about 15% of hadronically interacting DM (HIDM) with mass $\mathcal{O}$(GeV), whose trajectories intersect Earth, are captured. Ref. [13] develops in detail the theory of the HIDM atmosphere which forms around Earth, in the absence of hybridization. The number of SDM particles captured by Earth over its lifetime can be estimated in different ways. Here we use $N_S \approx 1.3 \times 10^{41}$ as calculated in [13], for an accumulation rate of

$$\dot{N}_S \approx 2.8 \times 10^{37} \text{ Myr}^{-1} . \tag{20}$$

$\dot{N}_S$ can arguably be up to a factor-6 higher [68], increasing proportionately all of the abundance estimates below. Here we give a very simplified treatment of the hybridization process, for some illustrative possibilities.

In a collision with the relatively massive nuclei comprising the Earth and its atmosphere, an energetic DM particle of mass $2m_p$ loses 4/9 of its energy, on average. To go from $v_{\rm esc} = 11$ km/s after the DM is gravitationally bound, to $v \approx 1$ km/s for thermal equilibrium at 300 K, requires of order 10 collisions – negligible compared to the total number of scatterings typically preceding a hybridization event. The mass of the DM is small relative to the nuclei it scatters on, and the velocities are very small, so the CM and lab frames are essentially the same and the scattering is isotropic in the lab frame.

As SDM diffuses through the atmosphere or in the Earth, two processes are at play:

1. The SDM *scattering length* is determined by its interaction with *all* of the nuclei in the local environment :

$$\bar{\lambda} = \left(n \sum_A f_A \, \sigma_A \right)^{-1} , \tag{21}$$

where f_A is the fractional abundance by number of nucleus A and n is the total number density. The total path length L while traversing a thickness z_0 is then, in homogenous diffusion approximation:

$$L = 3 \, z_0^2 / \bar{\lambda} = \bar{\lambda} \, N_{\rm scat} , \tag{22}$$

where the last relationship enables the mean number of scatterings in the medium to be deduced.

2. The SDM *capture length* is determined by its capture cross section on those nuclei with $A \geq A_{\min}$ capable of forming bound states ($A_{\min}$ depends on α_{SN}, as shown in Fig. 12), giving:

$$\bar{\lambda}^{\rm cap} = \left(n \sum_{A \geq A_{\min}} f_A \, \sigma_A^{\rm cap} \right)^{-1} . \tag{23}$$

Capture occurs if $L \gtrsim \bar{\lambda}^{\rm cap}$.

Fig. 13 shows the scattering cross section versus α_{SN} for a number of interesting or abundant elements in the Earth's crust. For $\alpha_{SN} \geq 0.03$ (the minimum to bind ^{238}U), all SDM captured by Earth become bound to nuclei and the dewar limits discussed in Sec. VI B (and indeed all limits of [13]) are evaded. However the distribution over host elements and physically in the Earth, of the $\approx 1.3 \times 10^{41}$ S's accumulated over the Earth's lifetime, varies dramatically with the value of α_{SN}.

The simplest scenario to analyze is when DM predominantly captures on O in the ocean, which we discuss to illustrate the analysis; a more comprehensive study of other possibilities is presented in [68]. Natural O is predominantly ^{16}O, with 0.2% ^{18}O. Since the scattering and capture cross sections depend on A, not Z, these are not exactly equivalent regarding their capture probability, but we lump them together in this first, broad-brush description. Moreover the O in the atmosphere (which is mostly in O_2) rapidly cycles with O in the oceans and biomass on the timescales relevant to this problem, and furthermore the column number density of O in the atmosphere is small compared to that in H_2O in the ocean, so we lump together O from both atmosphere and ocean, for this simple treatment.

The oceans cover 70% of the Earth's surface, with mean depth 5 km and scattering length $\lambda = 30\,cm/\sigma_b$, for $N_{scat} \approx 10^{12}$ from Eq. (22). Thus SDM incident on the surface of the oceans will be captured by O in the ocean water, as long as an OS bound state exists and $\sigma_O^{cap}/\sigma_O \gtrsim 10^{-12}$. (For comparison, neutron capture cross sections are typically $10^{-4} - 10^{-5}$ times the scattering cross section; if this ratio were applicable to SDM, capture would take place after $\approx 10^{4-5}$ collisions, or a path length of $\lesssim 3$ km.) Ocean water has a residence time of ≈ 100 Myr, during which $0.7 \times 2.8 \times 10^{39}$ SDM particles capture. The total number of O nuclei in the oceans and atmosphere is 5.5×10^{46} for a fractional abundance of OS relative to all O of $\approx 5 \times 10^{-8}$.

If the capture to scattering cross section ratio is smaller than 10^{-12}, capture would not occur on first passage through the ocean and the OS would be distributed more uniformly through the solid Earth, since O is the most abundant element in rocks. Assuming OS bound states exist and O is the dominant binding site for the SDM, a lower limit on the fractional abundance is given by assuming it is distributed uniformly over all the O in the Earth:

$$\frac{N_{OS}}{N_O} \gtrsim \frac{1.3 \times 10^{41}}{6.7 \times 10^{49}} \approx 2 \times 10^{-9} \,. \qquad (24)$$

Comprehensive predictions of the distribution of captured SDM over different molecules and physical locations in Earth and its atmosphere, for general α_{SN}, will require a multidisciplinary effort.

C. Exotic isotope detection

The mass of the exotic isotope is

$$M_{AS} = M_A + m_S - BE_A(\alpha) \,, \qquad (25)$$

where $BE_A(\alpha)$ is the ground-state binding energy shown in Fig. 11 (replacing $\alpha_{SN} \to \alpha$ for brevity). Generally, $BE_A(\alpha)$ ranges from 0 to ≈ 10 MeV. The main uncertainty in predicting M_{AS} is in the value of m_S. Based on the discussion in earlier sections, m_S can be anticipated to be in the range 1800-2000 MeV. For our fiducial value $m_S \approx 2\,m_p$, the exotic isotope is similar in mass to the $A + 2$ isotope.

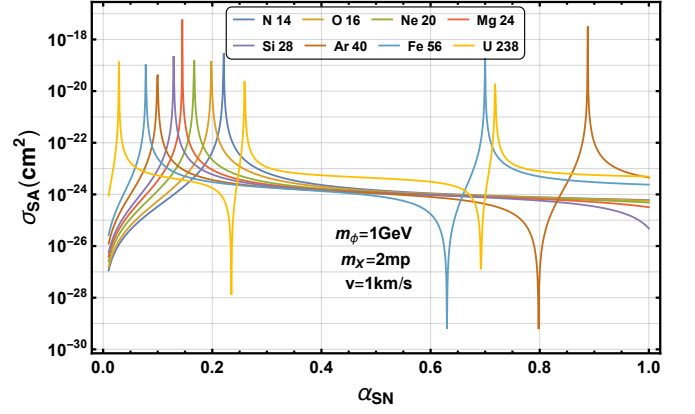^{18}O is a stable isotope which accounts for 0.2% of naturally occurring oxygen. If one in 10^9 of ^{16}O captures an SDM, that

FIG. 13: Cross section in cm^2 versus α_{SN} for selected nuclei $\{^{14}$N, ^{16}O, ^{20}Ne, ^{24}Mg, ^{28}Si, ^{40}Ar, ^{56}Fe, ^{238}U$\}$, for an attractive interaction. Below $\alpha_{SN} = 0.03$ there are no bound states for $A \leq 238$.

would produce an isotopic mass similar to naturally occurring ^{18}O at a ppm level which may well have gone unnoticed. Similarly the most abundant isotope of Si is ^{28}Si, but 3% of Si is ^{30}Si, potentially masking prior detection of the anomalous isotopic mass.

Modern mass spectroscopy tools used for geochemical research have the sensitivity and resolution to discover OS at the predicted level, with mass resolution in the $A \approx 16$ regime of at least 1 part in 30,000 (≈ 0.5 MeV) and up to 1 part in 1 million for certain specialized applications. [85, 86]. For smaller α_{SN} the threshold A_{min} for forming exotic isotopes increases, and estimating the abundance is more complex due to the non-trivial geochemistry of the Earth's crust. On the other hand, heavier nuclei are rarer so the fraction which are exotic would be higher, so robust limits on $\alpha_{SN} \gtrsim 0.04$ may be possible through dedicated searches.

Although predicting the abundances of different exotic isotopes for general α_{SN} is challenging, the absence of comprehensive and accurate fractional abundance predictions does not preclude an effective experimental search. A potential signal is a narrow line in a sensitive mass spectrometer at a mass not known to be associated with known isotopes. Let us denote the mass of the unexplained line as μ_Z. Initial searches would focus on mass ranges $\mu_Z = M_{Z,A_i} \pm (1800 - 2000)$ MeV, where i denotes a stable isotope of Z. There are a number of signatures to discriminate a real sexaquark bound state signal from noise or other sources. If it is a bound state of $\{Z, A\}$ and sexaquark, then

$$\mu_Z = M_{Z,A} + m_S - BE_A(\alpha) \,. \qquad (26)$$

There is no ambiguity as to which $\{Z, A_i\}$ could be the bound state host nucleus because the range of mass uncertainty, 100 MeV, $<< 1$ amu.

Three complementary classes of consistency conditions are:

● Multiple stable isotopes $\{Z, A_i\}$

Each isotope of the same element should have a similar relative abundance of SDM bound states, to the extent that their

geochemical history is the same and α_{SN} is not near a resonance for this A range (which can lead to significant differences in $\sigma^{\rm cap}_{Ai,Aj}$). Thus a line of similar strength should be found associated with each stable isotope, with the line positions satisfying

$$\mu_{Z,i} - \mu_{Z,j} = M_{Z,A_i} - M_{Z,A_j} - BE_{A,i}(\alpha) - BE_{A,j}(\alpha) . \tag{27}$$

Except near a resonance value for $\{A, \alpha\}$, BE is a slowly varying function of A so the splitting in Eq. (27) is generically small, $\lesssim 1$ MeV. To the extent that the exotic abundances are the same, the line strengths relative to those of the unbound isotopes should be similar.

- Hosts with neighboring $\{Z, Z'\}$

If elements can be studied which have neighboring $\{Z, Z'\}$ with both having stable isotopes with the same A, the prediction is even stronger:

$$\mu(Z, A) \approx \mu(Z', A) \tag{28}$$

with the equality only broken due to non-identical nuclear wavefunctions of $\{Z, A\}$ and $\{Z', A\}$. Here, however, the fractional abundances and hence signal strength are not in general the same, since the geophysics and geochemistry of the two elements is different.

- Multiple observed lines for different $\{Z, A\}$ hosts

With signals seen for $N \geq 3$ different $\{Z, A\}$ hosts, one can extract $m_S - BE(A)$ for each of them. Within the uncertainty on $BE_A(\alpha)$ due to uncertainties in the nuclear wavefunctions, a single value of m_S and α_{SN} should give a good fit to all $\mu_{Z,A}$.

IX. ACCELERATOR SEARCHES FOR THE SEXAQUARK

One of us (GRF, [2]) made a comprehensive review of experimental searches for the H-dibaryon and determined that apart from one experiment, all of the searches up to 2017 either searched for decay products or were only sensitive to masses below 2 GeV, making them insensitive to the hypothesized stable S. The one exception, BNL E888 [87], placed bounds that were far too weak to be relevant to its existence [2]. The experimental challenge to discovering an S and demonstrating its existence is that S's are similar in mass to neutrons, but interact less and are much less abundant. In a low energy exclusive reaction such as $K^- p \to S \bar{\Lambda}$, the quantum numbers of the unseen S are unambiguous, but the rate S production $\sim \tilde{g}^2$. If the DM is composed of sexaquarks, $\tilde{g}^2 \lesssim 4 \times 10^{-12}$ (see Sec. III C), and the expected suppression is even more severe if the theoretical estimate for $\tilde{g}$ (Sec. IV A) is used.

The situation in a high energy collision is different, and we must consider two regimes. In an inclusive short-distance-initiated reaction like decay of Upsilon(1S,2S,3S), closure approximation is valid and estimation is relatively robust. The

analysis is given in [2] and recapped in Supplemental Materials XII B 2. Estimating the S:n production ratio in the central region of high energy collision is more uncertain. One approach is to use the naive rule of thumb based on baryons versus mesons that for each additional quark which has to be incorporated into a hadron, the abundance is reduced by a factor 10-20. Producing an S entails 3 additional quarks that must be incorporated into the state, for a penalty of a factor 10^3, and baryon number conservation requires the production of still another anti-baryon relative to the case of neutron production, for an additional penalty of 10^{1-3} depending on how that should be counted. Since no penalty is imposed on account of the S's small size this may be an overly optimistic estimate, but it suggests that in a very high energy collision or in the final state of Z decay, the abundance of S's (or $\bar{S}$'s) could be $10^{-4} - 10^{-6}$ relative to neutrons.

However it is not enough to produce an S – it must be identified, or its presence unambiguously established, which is non-trivial. Unlike in a search for heavy Beyond the Standard Model neutral particles, e.g., as expected in Supersymmetry [88], the S has a typical QCD transverse momentum, $\mathcal{O}(1)$ GeV, so the missing energy or missing transverse momentum it carries is too small to notice at a high-energy accelerator. Two methods to search were suggested in [2]: searching the final states of Υ decay and searching for a very distinctive signature of $\bar{S}$ annihilation at the LHC. They are briefly recalled below along with several new suggestions.

- Final states of $\Upsilon(1S, 2S, 3S)$ decays

  The reactions

$$\Upsilon\ [\to \text{gluons}] \to S\, \bar{\Lambda}\bar{\Lambda}\ \text{ or }\ \bar{S}\, \Lambda\Lambda\ + \text{pions and/or}\ \gamma \tag{29}$$

are ideal discovery channels. The characteristic size of the ggg state from which the final hadrons emerge is $(10 \text{ GeV})^{-1} = 0.02$ fm, so the small size of the S is not an inherent disadvantage, as it is when produced in a reaction like $K^- p \to S\bar{\Lambda}$. A statistical estimate of the branching fraction for *inclusive* S plus $\bar{S}$ production is 2.7×10^{-7}; see the Supplemental Materials for details. It is small due to the necessity of producing extra gluons to have the required minimum 6 $q\bar{q}$ pairs, and the low probability of 6 quarks or antiquarks of the required flavors being in a color-flavor-spin singlet state.

If all of the final particles are seen, the mass of the unseen S can be reconstructed from 4-momentum conservation: $m_S^2 = (p_\Upsilon - p_{\Lambda 1} - p_{\Lambda 2} - \Sigma p_{\pi's\&\gamma})^2$. The width of the missing-mass peak is entirely due to resolution which is so good in some detectors, $\mathcal{O}(20)$ MeV, that even a few events appearing to be $\bar{\Lambda}\bar{\Lambda}$ or $\Lambda\Lambda$ + pions or gamma, having a common missing mass, would be a powerful smoking gun for the existence of the S and would accurately determine its mass. The initial state can be any Υ or continuum state below open-bottom threshold. Other final states besides $\Lambda\Lambda/\bar{\Lambda}\bar{\Lambda}$ are also discovery avenues, e.g., $\Xi^- p$, or a Λ can be replaced by $K^- p$. As long as no B- and S-carrying particle escapes detection besides the S or $\bar{S}$, any combination of hyperons and mesons with B= $\pm$ 2, S= $\mp$ 2 quantum numbers, including final states with higher multiplicities, can be used. The $\bar{\Lambda}\bar{\Lambda}$ and $\Lambda\Lambda$ final states are very good because the Λ's short decay length ($c\tau = 8$ cm) and

64% branching fraction to the 2-body charged final state $p\,\pi^-$, means Λ's and $\bar{\Lambda}$'s can be reconstructed with high efficiency, and their 4-momenta well-measured.

Babar performed a search for *exclusive* S and $\bar{S}$ production and placed an upper limit on the branching fraction of $\mathrm{BF_{exc}} < 1 - 2 \times 10^{-7}$ [89]. However as is shown in the Supplemental Materials by examining exclusive branching fractions for other channels in Υ decay, the penalty for demanding an exclusive final state is at least a factor 10^4. Thus Babar's sensitivity in the search [89], is by far insufficient to shed light on the possible existence of a stable S. (The utility of Υ decay final states as being potentially enriched in flavor-singlets, in particular the H-dibaryon, was recognized early-on by Belle, however their search [90] assumed the H-dibaryon was unstable and sought evidence of its decay into Λ final states, so is inapplicable to the sexaquark scenario.)

A more general strategy than just identifying events with exactly two Λs or two $\bar{\Lambda}$s plus only pions or gammas in final states of $\Upsilon(1S, 2S, 3S)$ decay, is to study the proportion of events having specified numbers $\{N_B, N_S, N_{\bar{B}}, N_{\bar{S}}\}$ of baryons, strangeness +1 particles, anti-baryons and strangeness -1 particles, respectively, in the final state. The feasibility of establishing a statistically significant excess of events with the correlated $N_B - N_S = \pm 4$ expected in the case of S and $\bar{S}$ production, depends on N_{tot}, the total number of $\Upsilon(1S, 2S, 3S)$ decays recorded, and the ID efficiency of the various baryons and strange particles, including losses from less than 4π detector coverage. In the Supplemental Materials a simple estimate is given, using a single effective efficiency for identifying baryons and anti-baryons, e_B, and similarly e_S for strange and anti-strange particles, to roughly assess the feasibility. It suggests that the estimated inclusive branching fraction 2.7×10^{-7} may be accessible to Belle-II, depending on the amount of running on $\Upsilon(1S, 2S, 3S)$ and the actual effective efficiencies. This motivates a more detailed investigation with a real detector simulation. The hadronic event generator EPOS-LHC has been modified to incorporate S and $\bar{S}$ production in hadron and heavy ion collisions, and in $\Upsilon(1S, 2S, 3S)$ decay, with a coalescence model production mechanism [91].

● $\bar{S}$ annihilation in an LHC tracker

With some rate, perhaps $10^{-4} - 10^{-6}$ relative to neutrons according to the simplistic estimate above, $\bar{S}$'s should be produced in LHC collisions. In a detector such as CMS, ATLAS, ALICE or LHCb, such an $\bar{S}$ can annihilate with a nucleon in the material of the beam-pipe or tracker, to produce a very distinctive final state in which for instance a $\bar{\Lambda}$ and a K emerges from the material. Unfortunately, the expected rate of useful events is very small. If the lab energy of the $\bar{S}$ is small enough for the annihilation event to not produce too many final particles, the cross section $\sim \tilde{g}^2$, i.e., very small. If the energy is large and many particles are produced, possibly evading the breakup amplitude suppression, then identifying the characteristic B = -1 and S = +2 signature of the final state is almost hopeless. See [2] for more detailed discussion.

● Search for long-interaction-length stable neutral particle

The challenge in searching for inclusive S and $\bar{S}$ production in a high energy collision is the problem of identifying them in the face of vastly more neutrons, as mentioned earlier. A possible strategy is to search for evidence of a neutral component with interaction length longer than that of neutrons and different from known neutral long-lived particles. Due to the small value of $\tilde{g}$, the $\bar{S}$ annihilation channel is much smaller than its scattering channel, so $\bar{S}$ interactions should be very similar to S interactions. The S and $\bar{S}$'s are generally relativistic even in the central region, so the calculations in Sec. V do not apply. Instead, we can roughly estimate their interaction length relative to that of neutrons in this energy regime as $\lambda_S^{\mathrm{int}} \approx (\alpha_{NN}/\alpha_{SN})^2\, \lambda_n^{\mathrm{int}} \approx 6 \times 10^3\, (0.2/\alpha_{SN})^2\, \lambda_n^{\mathrm{int}}$, with coupling α_{SN} taken to be the same to first approximation as the α_{SN} which enters the potential scattering problem relevant for dark matter constrained in Sec. V.

The strategy of looking for an anomalous component of long-interaction-length neutral stable particles could be implemented with a relatively simple customized experiment. Conceptually, a beam is directed onto a target, followed by sweeping magnets and decay region to eliminate charged particles and short-lived neutral components. This would be followed by an instrumented region with particle tracking interleaved with absorber, whose overall length is $\gtrsim 10^5$ neutron interaction lengths. The requirements on the tracking being to measure the longitudinal position of n- and S- or $\bar{S}$- initiated events, and to discriminate between interactions and decays, which need to be rejected. A quasi-beam-dump setup could be employed to reduce the $n : S$ ratio in the detector. The detector could be built up in stages, initially adapted to a shorter interaction length in case α_{SN} is larger than 0.2. An in-principle-complementary approach is exemplified by the experiment of [92] at Fermilab which used timing rather than anomalous interaction length. It was only sensitive to masses above 2 GeV due to neutron background, so not applicable for the sexaquark. However the method requires measuring the energy deposit and time-of-flight to discriminate the new particle from neutrons so seems to be both more complicated and less powerful – but perhaps merits consideration.

● Heavy Ion Collisions

A very attractive production channel for S and $\bar{S}$ is in the central region of relativistic heavy ion collisions (HICs), because of the similarity of the production to that of DM in the Early Universe. The process is not identical to the Early Universe because in the Early Universe the cooling timescale at the hadronization transition is $\sim 10^{-5}$s and the medium is infinite, while in a heavy ion collision the cooling time is very much shorter and the plasma expands into the vacuum.

Ref. [17] obtains an excellent fit to the relative abundances of final particles in central Pb-Pb collisions, including such complex and exotic states as hyper-triton, assuming statistical equilibrium at a temperature $T = 156$ MeV and accounting for production and decays of resonances. The main systematic uncertainty is associated with treatment of the resonances. A similar approach applied to S and $\bar{S}$ production would give a result similar to deuteron and anti-deuteron: $dN/dY \approx 10^{-1}$ in the central Pb-Pb collisions at $\sqrt{s_{NN}} = 2.76$ TeV – about

a factor-300 less than p and $\bar{p}$.

Perhaps the long-interaction-length neutral particle technique can be employed, depending on the particulars of the detector. Another strategy is to look for an excess of events in which the observed final state has baryon number minus strangeness $|B - S| = 4$, due to production and escape of an S or $\bar{S}$ whose baryon number and strangeness is balanced by the observed final state hadrons. The problem of course is the impossibility of perfectly measuring the B and S of each final particle. A further problem for ALICE is the limited rapidity range that can be observed. In Ref. [93], ALICE presents a study of the event-to-event fluctuations in the baryon number of particles with $0.6 < p < 1.5$ GeV/c and $|\eta| < 0.8$. For central collisions the difference in number of baryons and anti-baryons is of order the sum. With such large fluctuations, it would appear difficult to discern a population of events above background with $B - S = \pm 4$, unless a large portion of the final particles can be ID'd. A detector simulation or an analysis along the lines of Supplemental Materials XIII would be needed to properly assess the prospects.

- High intensity photon beams

J-Lab has a tagged photon beam of energy 9 to 12 GeV, with 10^8 photons/second on target. The GlueX experiment anticipates collecting $\approx 10^{12}$ interactions. It has adequate kinematic reach to probe reactions such

$$\gamma p \rightarrow S \bar{\Lambda} K^+ + pions \,. \tag{30}$$

A 12 GeV photon provides $E_{\rm CM} = 4.84$ GeV; this is 1.35 GeV above the 3.5 GeV total mass of S, $\bar{\Lambda}$, K^+ for the fiducial $m_S = 2m_p$, leaving room to spare for phase space and pion production. Depending on the solid angle coverage and tagging efficiency, unbalanced baryon number and strangeness due to an escaping S could be a good discovery channel in spite of the S production rate going as $\sim \tilde{g}^2$, given the potentially very large number of events.

X. SUMMARY

At this point in time, it is not possible to decide on theoretical grounds whether there is an as-yet-undiscovered stable neutral boson with baryon number 2 in the QCD spectrum. Many would argue against this possibility based on faith in the qualitative and semi-quantitative understanding the community has developed of chiral symmetry breaking, quark confinement, asymptotic freedom and many aspects of the hadron spectrum in QCD. However in the spirit that our understanding of QCD may not be as complete as we would like to think, and motivated by the lack of a compelling and viable alternative Dark Matter candidate, we have examined here whether a stable sexaquark can be excluded in light of present knowledge, and whether it would make a satisfactory DM particle.

We find that sexaquark dark matter is not presently excluded either by accelerator experiments, dark matter direct detection constraints, astrophysical constraints such as neutron stars and SN1987a, or cosmological constraints such as

the CMB and structure formation or primordial nucleosynthesis.

The sexaquark relic abundance after the transition from the quark gluon plasma to the hadronic phase is completely determined in freezeout approximation by statistical physics, known parameters of QCD and the sexaquark mass. The predicted value is $\Omega_{DM}/\Omega_b \approx 5$, with better than factor-2 accuracy. This in remarkable agreement with the observed value $\Omega_{DM}/\Omega_b = 5.3 \pm 0.1$. The analysis is given in Sec. III.

Whether this no-free-parameter result persists to low-temperatures depends on the amplitude to break up a sexaquark into two baryons, $\tilde{g}$, which we calculate in Sec. IV A. Three separate effects combine to suppress sexaquark breakup, the most important being the hard-core radius characterizing the short-distance repulsion of the baryon-baryon potential; we adopt the central value of the standard fits to data, $r_c = 0.4$ fm [26, 27]. Other sources of suppression are the small radius of the sexaquark and the QCD barrier to tunneling through the intermediate state. Predictions for $\tilde{g}$ for extreme choices of the parameters are shown in Fig. 3, where one sees that even with no tunneling suppression and taking the maximum r_S, the breakup amplitude is too small to destroy the abundance ratio set at the QGP-hadron transition.

We also constrained the allowed range of $\tilde{g}$ empirically, most importantly by using SNO data to obtain a limit on the deuteron beta decay lifetime: $\tau_D > 10^{29}$ yr. This gives the strongest and most robust experimental limit to date on the sexaquark breakup amplitude if the S is lighter than 1870 MeV. It improves on and superceeds the estimates derived in [6] for Oxygen decay in SuperK. The limits on $\tilde{g}$ are summarized in Fig. 3. The mass range 1870-1880 MeV is virtually unconstrained, but any mass above 1850 is currently comfortably compatible with the constraints, given theoretical estimates for the breakup amplitude.

Since the S is a particle in QCD, its scattering on baryons can be related to parameters of effective field theory. The scattering is primarily due to exchange of the flavor singlet linear combination of ω and ϕ vector mesons, here denoted V (Sec. V). Thus SDM interacts with baryons via a Yukawa potential with range $m_V^{-1} \approx 0.2$ fm. The main uncertainty in the calculation of DM-nucleus cross sections is the strength of the potential, α_{SN}, and its sign. At leading order this is determined by the coupling between S and V, g_{SSV}, with $|\alpha_{SN}| = |g_{SSV} g_{NNV}|/(4\pi)$; we consider $0.001 < \alpha_{SN} < 10$.

We developed the necessary theoretical infrastructure to interpret DM direct detection experiments when the DM has non-perturbative interactions with nucleons. Cross sections do not scale with atomic mass A in the manner widely assumed based on Born approximation, and the form factor for extended nuclei and the velocity dependence of DM-nucleus cross sections exhibit strong, highly non-trivial behavior. We treated these in detail by solving the Schroedinger equation. We obtained constraints on the Yukawa coupling parameter α_{SN} as a function of m_S implied by direct detection experiments and constraints on $\sigma_{\rm DM-p}$ from the CMB power spectrum.

The excluded regions for an attractive interaction are shown in Fig. 9; the boundaries in the repulsive case are smooth

but similar. For a repulsive interaction and $m_S \approx 2m_p$, the maximum Yukawa coupling is $|\alpha_{SN}|_{\max} \approx 0.004$ and $\sigma_{SN} \lesssim 10^{-29}\text{cm}^2$, taking the dewar limits [13, 58] at face value; see Sec. VI B for a discussion of a more conservative choice.

For an attractive interaction, α_{SN} can be as large as 0.7 and the phenomenology of SDM is very rich. The constraint $\alpha_{SN} < \approx 0.7$ is required to avoid that virtually all primordial ^{4}He is in the form of a bound state with an S whose mass is about 2 amu larger than normal ^{4}He. But for $\approx 0.7 > \alpha_{SN} \gtrsim 0.03$, SDM captured by Earth quickly binds to nuclei. For example, if $\alpha_{SN} \gtrsim 0.2$, SDM binds to oxygen nuclei in the Earth's oceans, crust and atmosphere, forming a roughly 100-part-per-billion abundance of exotic isotopes of O with a mass about 2 amu larger than the fundamental nuclear mass. Experimental searches for exotic isotopes have not explored such small mass offsets with adequate (ppb) sensitivity. Future searches of this type are well-motivated because $\alpha_{SN} \gtrsim 0.004$ seems natural so the dewar limits for the repulsive case suggest the S-baryon interaction is attractive.

XI. CONCLUSIONS

We have shown that sexaquarks are an excellent dark matter candidate. Their relic density is fixed by the physics of the transition from quark gluon plasma to hadrons and statistical physics and known parameters from QCD predicts the DM to baryon density ratio $\Omega_{DM}/\Omega_b \approx 5$, in excellent agreement with the observed value $\Omega_{DM}/\Omega_b = 5.3 \pm 0.1$.

The possible range of sexaquark coupling strength to baryons considered here, $0.001 \lesssim \alpha_{SN} \lesssim 10$, allows for a broad range of phenomenological behaviors. The SDM-proton scattering cross section may be $\sigma_{S\text{p}} \lesssim 10^{-29}\,\text{cm}^2$, which would have evaded detection and is compatible with all cosmological, astrophysical and laboratory bounds; for a repulsive SDM-baryon interaction this is the only option compatible with observational limits. However the DM-nucleon interaction is *a priori* equally likely to be attractive, in which case the phenomenological options are much richer.

The sexaquark dark matter hypothesis motivates the following experimental efforts:

• Search for exotic isotopes of $A > 4$ nuclei in the Earth, having a mass offset of $m_S - BE$, with $BE \lesssim 10\,\text{MeV}$, i.e., about 2 amu heavier than the host nucleus A. If the Yukawa coupling between SDM and nucleons is attractive and strong enough to bind to oxygen, $\gtrsim \mathcal{O}(\text{ppb})$ of oxygen nuclei should be exotic and have a mass within 10's or at most 100's of MeV of ^{18}O. For weaker Yukawa coupling only heavier nuclei bind, motivating the search for exotic isotopes of a diversity of ele-

ments. If DM proves to be composed of sexaquarks which can bind to nuclei, the study of the abundances of exotic isotopes will become a powerful tool for geoscience as well as a high-precision window on the sexaquark mass and its coupling to nucleons.

• Search in final states of $\Upsilon(1S, 2S, 3S)$ decay, and also in heavy ion collisions and at J-Lab, for the signature of S or $\bar{S}$ production. In Upsilon decay one can search for events with $\bar{\Lambda}\bar{\Lambda}$ or $\Lambda\Lambda$ and no accompanying baryon number or strangeness. Even a handful of events in which all particles except the unseen S or $\bar{S}$ are well-measured, could give a missing-mass peak that is a decisive signature. Another strategy would be an inclusive search for events with $B - S = \pm 4$.

• Search for the presence of a second component in the interaction-length distribution of stable neutral particles produced in the central region of relativistic heavy ion or other high energy collisions. Taking anti-deuterium production as a guide, the abundance of the S and $\bar{S}$ component in a heavy ion collision should be about 0.3% that of n and $\bar{n}$. The anomalous interaction length depends on α_{SN} which is constrained by cosmological and dewar constraints as discussed in Sec. V; a rough estimate is $\lambda_S^{\text{int}} \approx 6 \times 10^3 \, \lambda_n^{\text{int}} (\alpha_{SN}/0.2)^2$.

• Calibrate the XQC and other semi-conductor detectors used to search for DM with mass less than a few GeV, to determine the extent to which low energy recoiling atoms deposit their energy in forming lattice point defects (Frenkel pairs) or coherent phonon excitations (thermalization). If the fraction of energy thermalized is large enough, detectors such as XQC above the atmosphere or CRESST near the surface of Earth would be sensitive to DM mass in the $\approx 2m_p$ range. However until these detectors are calibrated for low recoil energies, they can only be used to place limits on DM interactions above the mass range relevant for SDM.

[1] P. A. R. Ade et al. (Planck Collaboration), Astron. Astrophys. **594**, A13 (2016), 1502.01589.
[2] G. R. Farrar (2017), 1708.08951v2.
[3] R. Jaffe, Phys. Rev. Lett. **38**, 195 (1977), nucl-th/9912031.
[4] G. R. Farrar (2018), 1805.03723.
[5] M. Tanabashi et al. (Particle Data Group), Phys. Rev. **D98**, 030001 (2018).
[6] G. R. Farrar and G. Zaharijas, Phys. Rev. **D70**, 014008 (2004), hep-ph/0308137.
[7] S. Raby, S. Dimopoulos, and L. Susskind, Nucl. Phys. **B169**, 373 (1980).
[8] T. Hatsuda, Front. Phys.(Beijing) **13**, 132105 (2018).

[9] T. Yamazaki and Y. Kuramashi, Phys. Rev. **D96**, 114511 (2017), 1709.09779.

[10] Z. Davoudi, EPJ Web Conf. **175**, 01022 (2018), 1711.02020.

[11] S. Acharya et al. (ALICE), Phys. Lett. **B797**, 134822 (2019), 1905.07209.

[12] G. Baym, E. W. Kolb, L. D. McLerran, T. P. Walker, and R. L. Jaffe, Phys. Lett. **160B**, 181 (1985).

[13] D. A. Neufeld, G. R. Farrar, and C. F. McKee, Astrophys. J. **866**, 111 (2018), 1805.08794.

[14] T. Bhattacharya et al., Phys. Rev. Lett. **113**, 082001 (2014), 1402.5175.

[15] A. Bazavov et al. (2018), 1802.04248.

[16] A. De Rujula, H. Georgi, and S. L. Glashow, Phys. Rev. **D12**, 147 (1975).

[17] A. Andronic, P. Braun-Munzinger, K. Redlich, and J. Stachel, Nature **561**, 321 (2018), 1710.09425. It should be noted that other models have been put forward to fit the HIC data, including, e.g., J. Cleymans et al, Phys. Rev. C **84** (2011) 054916 and K. A. Bugaev et al., e-Print: 2005.01555.

[18] C. M. Ko, V. Koch, and G.-Q. Li, Ann. Rev. Nucl. Part. Sci. **47**, 505 (1997), nucl-th/9702016.

[19] G. R. Farrar and N. Wintergerst (2020), in preparation.

[20] V. G. J. Stoks and T. A. Rijken, Nucl. Phys. **A613**, 311 (1997), nucl-th/9611002.

[21] M. Cannoni, Int. J. Mod. Phys. **A32**, 1730002 (2017), 1605.00569.

[22] E. W. Kolb and M. S. Turner (2018), 1809.06003.

[23] C. Gross, A. Polosa, I. A. Strumia, A. Urbano, and W. Xue (2018), 1803.10242.

[24] S. D. McDermott, S. Reddy, and S. Sen (2018), 1809.06765.

[25] N. Bar, K. Blum, and G. D'amico (2019), 1907.05020.

[26] T. Hamada and I. D. Johnston, Nucl. Phys. **34**, 382 (1962).

[27] R. V. Reid, Jr., Annals Phys. **50**, 411 (1968).

[28] K. Sasaki et al., PoS **LATTICE2016**, 116 (2017), 1702.06241.

[29] Z. Wang and G. R. Farrar, in preparation (2020).

[30] J. K. Ahn et al., Phys. Rev. Lett. **87**, 132504 (2001).

[31] H. Takahashi et al., Phys. Rev. Lett. **87**, 212502 (2001).

[32] G. R. Farrar and G. Zaharijas, Phys. Rev. **D70**, 014008 (2004), hep-ph/0308137.

[33] G. R. Farrar, Phys. Rev. Lett. submitted (2017).

[34] A. Bellerive, J. R. Klein, A. B. McDonald, A. J. Noble, and A. W. P. Poon (SNO), Nucl. Phys. **B908**, 30 (2016), 1602.02469.

[35] R. Essig, E. Kuflik, S. D. McDermott, T. Volansky, and K. M. Zurek, JHEP **11**, 193 (2013), 1309.4091.

[36] T. R. Slatyer and C.-L. Wu, Phys. Rev. **D95**, 023010 (2017), 1610.06933.

[37] P. M. M. Maessen, T. A. Rijken, and J. J. de Swart, Phys. Rev. **C40**, 2226 (1989).

[38] M. M. Nagels, T. A. Rijken, and Y. Yamamoto, Phys. Rev. **C99**, 044003 (2019), 1501.06636.

[39] X. Xu and G. R. Farrar, in preparation (2020).

[40] S. Tulin, H.-B. Yu, and K. M. Zurek, Phys. Rev. D **87**, 115007 (2013), 1302.3898.

[41] M. R. Buckley and P. J. Fox, Phys. Rev. D **81**, 083522 (2010), URL https://link.aps.org/doi/10.1103/PhysRevD.81.083522.

[42] D. McCammon et al., Astrophys. J. **576**, 188 (2002), astro-ph/0205012.

[43] G. Zaharijas and G. R. Farrar, Phys. Rev. **D72**, 083502 (2005), astro-ph/0406531.

[44] A. L. Erickcek, P. J. Steinhardt, D. McCammon, and P. C. McGuire, Phys. Rev. **D76**, 042007 (2007), 0704.0794.

[45] M. Shafi Mahdawi and G. R. Farrar, JCAP **12**, 004 (2017),

[46] M. S. Mahdawi and G. R. Farrar, JCAP **1810**, 007 (2018), 1804.03073.

[47] Y. Bar-Yam and J. D. Joannopoulos, Phys. Rev. Lett. **52**, 1129 (1984).

[48] M. Tang, L. Colombo, J. Zhu, and T. Diaz de la Rubia, Phys. Rev. B **55**, 14279 (1997), URL https://link.aps.org/doi/10.1103/PhysRevB.55.14279.

[49] W. K. Leung et al., Phys. Rev. Lett. **83**, 2351 (1999).

[50] M. Huhtinen, Nucl. Instrum. Meth. **A491**, 194 (2002).

[51] J. R. Srour, C. J. Marshall, and P. W. Marshall, IEE Trans. Nucl. Sci. **50**, 653194 (2003).

[52] P. Rinke et al., Phys. Rev. Lett. **102**, 026402 (2009).

[53] V. Gusakov, V. Belko, and N. Dorozhkin, Physica B **404**, 4558 (2009).

[54] A. Junkes, Ph.D. thesis, Hamburg U. (2011), URL http://www-library.desy.de/cgi-bin/showprep.pl?thesis11-031.

[55] E. R. Dobrovinskaya et al., Sringer Science + Business Media, LLC (2009).

[56] V. A. J. van Lint, T. M. Flanagan, R. E. Leadon, J. A. Naber, and V. C. Rogers, NASA STI/Recon Technical Report A **81**, 13073 (1980).

[57] W. L. Xu, C. Dvorkin, and A. Chael, Phys. Rev. **D97**, 103530 (2018), 1802.06788.

[58] D. A. Neufeld and D. J. Brach-Neufeld, Astrophys. J. **877**, 8 (2019), 1904.01590.

[59] E. O. Nadler, V. Gluscevic, K. K. Boddy, and R. H. Wechsler, Astrophys. J. **878**, L32 (2019), [Astrophys. J. Lett.878,32(2019)], 1904.10000.

[60] D. Wadekar and G. R. Farrar, arXiv e-prints arXiv:1903.12190 (2019), 1903.12190.

[61] D. Spergel and P. Steinhardt, Phys. Rev. Lett. **84**, 3760 (2000), astro-ph/9909386.

[62] M. Boylan-Kolchin, J. S. Bullock, and M. Kaplinghat, MNRAS **415**, L40 (2011), 1103.0007.

[63] D. H. Weinberg, J. S. Bullock, F. Governato, R. Kuzio de Naray, and A. H. G. Peter, Proceedings of the National Academy of Science **112**, 12249 (2015), 1306.0913.

[64] P. Creasey, O. Sameie, L. V. Sales, H.-B. Yu, M. Vogelsberger, and J. Zavala, MNRAS **468**, 2283 (2017), 1612.03903.

[65] T. Ren, A. Kwa, M. Kaplinghat, and H.-B. Yu, Phys. Rev. **X9**, 031020 (2019), 1808.05695.

[66] S. Tulin and H.-B. Yu, Phys. Rept. **730**, 1 (2018), 1705.02358.

[67] J. E. Lynn, Theory of Neutron Resonance Reactions (Clarendon Press-Oxford, 1968).

[68] G. R. Farrar, X. Xu, and J. Eiler, in preparation (2020).

[69] S. Riemer-Srensen and E. S. Jenssen, Universe **3**, 44 (2017), 1705.03653.

[70] B. D. Fields, Ann. Rev. Nucl. Part. Sci. **61**, 47 (2011), 1203.3551.

[71] B. D. Fields, P. Molaro, and S. Sarkar, Chin. Phys. **C40** (2017).

[72] M. Asplund, D. L. Lambert, P. E. Nissen, F. Primas, and V. V. Smith, Astrophys. J. **644**, 229 (2006), astro-ph/0510636.

[73] L. Sbordone, P. Bonifacio, E. Caffau, H.-G. Ludwig, N. T. Behara, J. I. González Hernández, M. Steffen, R. Cayrel, B. Freytag, C. van't Veer, et al., Astronomy & Astrophys. **522**, A26 (2010), 1003.4510.

[74] A. Coc and E. Vangioni, International Journal of Modern Physics E **26**, 1741002 (2017), 1707.01004.

[75] P. Molaro and J. Beckman, Astronomy & Astrophys. **139**, 394 (1984).

[76] M. Spite, P. Bonifacio, F. Spite, E. Caffau, L. Sbordone, and A. J. Gallagher, Astronomy & Astrophys. **624**, A44 (2019),

1902.11048.

[77] R. A. Muller, L. W. Alvarez, W. R. Holley, and E. J. Stephenson, Science **196**, 521 (1977).

[78] P. F. Smith and J. R. J. Bennett, Nucl. Phys. **B149**, 525 (1979).

[79] P. F. Smith, J. R. J. Bennett, G. J. Homer, J. D. Lewin, H. E. Walford, and W. A. Smith, Nucl. Phys. **B206**, 333 (1982).

[80] T. K. Hemmick et al., Phys. Rev. **D41**, 2074 (1990).

[81] D. Javorsek, D. Elmore, E. Fischbach, D. Granger, T. Miller, D. Oliver, and V. Teplitz, Phys. Rev. Lett. **87**, 231804 (2001).

[82] D. Javorsek, D. Elmore, E. Fischbach, T. Miller, D. Oliver, and V. Teplitz, Phys. Rev. **D64**, 012005 (2001).

[83] P. Mueller, L. B. Wang, R. J. Holt, Z. T. Lu, T. P. O'Connor, and J. P. Schiffer, Phys. Rev. Lett. **92**, 022501 (2004), nucl-ex/0302025.

[84] G. Zaharijas and G. R. Farrar, Phys.Rev. **D72**, 083502 (2005).

[85] J. M. Eiler et al., Int. J. Mass Spectrometry **335**, 45 (2013).

[86] J. M. Eiler et al., Int. J. Mass Spectrometry **422**, 126 (2017).

[87] J. Belz et al. (BNL-E888), Phys. Rev. **D53**, R3487 (1996).

[88] G. R. Farrar and P. Fayet, Phys. Lett. **76B**, 575 (1978).

[89] J. P. Lees et al. (BaBar) (2018), 1810.04724.

[90] B. Kim et al. (Belle), Phys. Rev. Lett. **110**, 222002 (2013), 1302.4028.

[91] T. Pierog et al. (2020), in preparation.

[92] H. Gustafson et al., Phys. Rev. Lett. **37**, 474 (1976).

[93] S. Acharya et al. (ALICE) (2019), 1910.14396.

[94] N. K. Glendenning and J. Schaffner-Bielich, Phys. Rev. **C58**, 1298 (1998), astro-ph/9803232.

[95] D. Blaschke, S. Typel, M. Shahrbaf, D. Alvarez, and G. R. Farrar, Compatibility of Compact Star properties with Sexaquarks, in preparation (2020).

[96] C. Kouvaris and P. Tinyakov, Physical Review Letters **107**, 091301 (2011), 1104.0382.

[97] S. D. McDermott, H.-B. Yu, and K. M. Zurek, Phys. Rev. D **85**, 023519 (2012), 1103.5472.

[98] N. F. Bell, A. Melatos, and K. Petraki, Phys. Rev. D **87**, 123507 (2013), 1301.6811.

[99] R. Brito, V. Cardoso, C. F. B. Macedo, H. Okawa, and C. Palenzuela, Phys. Rev. D **93**, 044045 (2016), 1512.00466.

XII. SUPPLEMENTAL MATERIALS

A. Neutron Star Equation of State

The discovery of several neutron stars (NS) with masses greater than $2M_\odot$ presents a great challenge to hadron physics. Allowing just for known hadronic degrees of freedom – nucleons, hyperons and mesons – the equation of state (EoS) is too soft to support a NS of such a large mass against collapse to a black hole. One option to explain this observation is to invoke a transition from hadronic to quark degrees of freedom, where the freedom in our knowledge of the quark EoS allows higher masses than possible in the hadronic phase.

It has been known for some time that the presence of an H-dibaryon exacerbates the problem of NS masses and would exclude $M_{\rm NS} = 1.4M_\odot$; indeed this was an argument against the existence of the H-dibaryon [94] . The point is that being a boson there is no Fermi pressure support for an H-dibaryon component, unlike when the same state is dissociated into two Λ's. With a sexaquark the analysis is similar to that for an H-dibaryon. A Λ converts to an S via $\Lambda n \rightarrow S$ in $\mathcal{O}(\rm hr)$, in spite of the small cross-section $\sim (G_F \tilde{g})^2$, due to the very high density of n's. The strong interaction process $\Lambda\Lambda \rightarrow S$ has a factor 10^{12} times higher rate and will dominate except when the Λ density is low. Therefore, when chemical equilibrium calls for a component of S's, it will be present. Paradoxically, discovering even more massive NS's up to significantly $> 2M_\odot$ eliminates the NS argument against the H-dibaryon and the S: once the transition to a quark plasma must be accepted as established, the presence or absence of an H-dibaryon or S in the spectrum is largely irrelevant. Details will be discussed in [95].

Other papers arguing against bosonic dark matter based on NS stability against collapse to a BH [96–99] are not directly applicable to SDM with its repulsive self-interaction and the possibility of converting to strange quark matter in the core of the star.

B. $S/\bar{S}$ production in Υ decay

In the Appendix of [2], GF estimated a production fraction 2.7×10^{-7} for inclusive $S + \bar{S}$ production in the 3g channel at the Υ resonance, using a statistical model with no penalization for wavefunction overlaps. Babar has placed a limit on the branching fraction for the 3-body exclusive process $\Upsilon_{2,3S} \rightarrow S\bar{\Lambda}\bar{\Lambda}+cc$ of $(1.2-1.4)\times 10^{-7}$. The question addressed in this section is how constraining or not this limit on the exclusive production is. First, the statistical estimate for the inclusive branching fraction is given.

1. Statistical model for $S/\bar{S}$ production in Υ decay

All Υ decays below open-bottom, i.e., $\Upsilon(1S)$, $\Upsilon(2S)$ and $\Upsilon(3S)$ decays, go through 3-gluons. To leading order each gluon converts to q and $\bar{q}$s of ≈ 2 GeV, which produce mini-jets or form hadrons through string-fragmentation. Production

of the minimum $6q+6\bar{q}$ with 6 q's or $\bar{q}$'s having relatively similar momenta needed to produce an S or $\bar{S}$ requires creating 3 more gluons, at a penalty factor of α_s^3 in the amplitude. Here $\alpha_s \gtrsim \alpha_s(\Upsilon) \approx 0.2$, and may be $\mathcal{O}(1)$ because large momentum transfer is not required, so we adopt the geometric mean.

The next requirement is for 6 q or $\bar{q}$'s to be nearest neighbors in space, within a distance scale $< r_S$. Statistically, the penalty for having exclusively q's or $\bar{q}$'s within a nearest-neighbor grouping is $\left(\frac{1}{2}\right)^5$. As a zeroth approximation, no penalty is included for such a grouping of q or $\bar{q}$'s to have an appropriate spatial wavefunction to be an S or $\bar{S}$, on the grounds that the q and $\bar{q}$'s originate in a region of size $\approx \frac{1}{10\text{GeV}} = 0.02$ fm then expand, so at some point they will be in the relevant volume to form an S.

Finally, to form an S or $\bar{S}$, the 6 q's or $\bar{q}$'s must have the total flavor-spin-color quantum numbers to be an S or $\bar{S}$. Without loss of generality consider the $6q$ case. S belongs to the $(1,1,1)$ representation of $SU(3)_c \times SU(3)_f \times SU(2)_s$. With a spatially symmetric wavefunction, Fermi statistics implies it is in the totally antisymmetric 6-quark representation of $SU(18)$. In a statistical approximation that the q's produced by the gluons randomly populate all possible color, flavor and spin states, the fraction of cases contributing to the antisymmetric representation is $18 \times 17 \times 16 \times 15 \times 14 \times 13/(6 \times 5 \times 4 \times 3 \times 2)/18^6 = 5.46 \times 10^{-4}$. Dividing by 2^5, multiplying by $(\alpha_s^2 \approx 0.2)^3$ and by 2 for S and $\bar{S}$ results in the estimated branching fraction of Upsilon to states containing an S or $\bar{S}$: $\text{BF}_S \approx 2.7 \times 10^{-7}$.

A more detailed model calculation could give a larger estimate, since color correlations among the gluons and quarks likely enhance the amplitude for states corresponding to attractive QCD channels, while the simplification of ignoring the spatial structure could lead to a suppression. Combining these effects with the crude nature of the estimated dependence on α_s, means improvements can take this naive estimate in either direction.

2. Penalty for low-particle-number exclusive final states

We begin by noting some measured branching fractions that can provide guidance for the penalty of demanding a low-particle-number exclusive final state rather than a more inclusive one, and their implications:
J/Ψ:

- Branching fraction for inclusive $B\bar{B}$ production $\approx 10^{-2}$: *Making a pair of baryons + mesons is 100x harder than just making mesons.*

- $\text{BR}(\pi+\pi^-)/\text{BR}(\pi+\pi^-+X) \approx (1.5 \times 10^{-4})/(0.15) = 10^{-3}$ with X an observed exclusive mode: *Exclusive to inclusive penalty is at least 10^{-3}*. There is an angular momentum barrier but plenty of phase space, so no suppression there.

Υ_{1S}:

- Sum over 100 observed exclusive modes accounts for 1.2% of decays: *Average observed exclusive $\approx 10^{-4}$.*

state	mass (MeV)	width (keV)
J/Ψ	3096.9	92.9 ± 2.8
Υ_{1S}	9460.3	54
Υ_{2S}	10023.3	32 ± 2.6
Υ_{3S}	10355.2	20.3 ± 1.85

TABLE I: 1^{--} Charmonium and Bottomonium states, from [5] .

Final State	branching fraction	number events
hadrons	87.7%	
virt. γ + hadrons	13.5%	
ggg	64.1%	
γgg	8.8 %	
$\ell^+\ell^-$	$\approx 3 \times 2\%$	
$\pi^+\pi^-$	1.47×10^{-4}	
$2(\pi^+\pi^-)\pi^0$	4.1%	
$3(\pi^+\pi^-)\pi^0$	2.9%	
$4(\pi^+\pi^-)\pi^0$	0.9%	
$\rho\pi$	1.7%	
$2(\pi^+\pi^-\pi^0)$	1.6%	
$\pi^+\pi^- + X$	14.6 %	
$p\bar{p}$	2.1×10^{-3}	
$p\bar{p} + \{\pi^0, \pi^+\pi^-, \pi^+\pi^-\pi^0, \eta\}$	12.5×10^{-3}	
$\omega 2\pi^+ 2\pi^-$	8.6×10^{-3}	
$\omega\pi^+\pi^-\pi^0, \omega\pi^0\pi^0$	$4.0, 3.4 \times 10^{-3}$	
$\pi^+\pi^-\pi^0, \phi K^+K^-, K^+K_S^0\pi^-$	$\approx 2 \times 10^{-6}$	
$\pi^+\pi^- 2\pi^0$	1.3×10^{-5}	
$\Xi^0\bar{\Xi}^0, \Delta(1232)^{++}\Delta(\bar{1}232)^{--}$	$1.7, 1.1 \times 10^{-3}$	

TABLE II: J/Ψ_{1S}, from [5]

- There is no observed 2-body decay, with upper limit 4×10^{-6}. (The most sensitive channels are $\rho\pi, \omega\pi$.) A few 3-body decays observed, biggest being $\omega\pi^+\pi^-$ with BR 4.5×10^{-6}: *Multi-body final states favored over 3-body. Suppression factor for 3-body may be as small as $\mathcal{O}(10^{-5})$.*

- Biggest identified exclusive decay, $\Upsilon_{1S} \to \pi^+\pi^- 2\pi^0$, has BR 1.3×10^{-5}.

$\Upsilon_{2S}, \Upsilon_{3S}$:

- $\text{BR}(\Upsilon_{2S} \to \Upsilon_{1S} + \pi\pi) = 26.5\%$.

- $\text{BR}(\Upsilon_{3S} \to \Upsilon_{2S} + X) = 0.1$.

- Several exclusive 3 body decays seen. The most significant is $\phi K^+ K^-$ with BR 1.6×10^{-6}.

- There are only upper limits on Υ_{2S} 2-body decays, except $K^*(892)^0 \bar{K}_2^*(1430)^0 + c.c.$ with BR= $(1.5 \pm 0.6) \times 10^{-6}$.

We need to estimate $\text{BF}(\Upsilon_{2,3S} \to S\bar{\Lambda}\bar{\Lambda})$. We can do that by starting from the observed $\text{BF}(\Upsilon_{1,2,3S} \to \phi K^+ K^-) \approx 2 \times 10^{-6}$ in all three cases. As for the inclusive $ggg \to S+X$, the rate for the exclusive process $\Upsilon_{2,3S} \to S\bar{\Lambda}\bar{\Lambda}$ is suppressed relative to $\Upsilon_{1,2,3S} \to \phi K^+ K^-$ by the factors

1. $(\alpha_s^2 \approx 0.2)^3 = 0.008$, to account for the production of 3 additional $q\bar{q}$ pairs beyond the 3 $q\bar{q}$ pairs required to form any non-exotic hadronic final state from ggg and in particular sufficient to form $\phi K^+ K^-$.

Final State	branching fraction	number events
ggg	81.7%	
γgg	2.2 %	
$\ell^+\ell^-$	$\approx 3 \times 2\%$	
$\rho\pi,\ \omega\pi$	$<\approx 3.7 \times 10^{-6}$	90%CL
$\pi^+\pi^-,\ K^+K^-,\ p\bar{p}$	$< 5 \times 10^{-4}$	90%CL
$\pi^+\pi^-\pi^0,\ \phi K^+K^-\ (\omega\pi^+\pi^-)$	$\approx 2(4.5) \times 10^{-6}$	also $KK\pi$
$\pi^+\pi^-\,2\pi^0$	1.3×10^{-5}	
sum 100 exc. modes	1.2 %	
$J/\Psi + X$	$(5.4 \pm 0.4) \times 10^{-4}$	

TABLE III: Selected Υ_{1S} hadronic decays, from [5]

Final State	branching fraction	number events
ggg	58.8%	
γgg	8.8 %	
$\Upsilon(1S) + \pi\pi$	26.5 %	
J/Ψ+anything	$< 6 \times 10^{-3}$	90% CL
$\pi^+\pi^-2\pi^0$	$1.3 \pm 0.3 \times 10^{-5}$	
ϕK^+K^-	$(1.6) \pm 0.4) \times 10^{-6}$	
$K^*K^-\pi^+$	$(2.3 \pm 0.7) \times 10^{-6}$	
$K_S^0 K^+\pi^- + cc$	1.14×10^{-6}	

TABLE IV: Selected Υ_{2S}, from [5]

2. $(1/2)^5 = 0.03$, the probability of having 6q's or 6$\bar{q}$'s in immediate proximity to make an S or $\bar{S}$. The parallel factor for the $\phi K^+ K^-$ final state is a factor $(1/2)^1 = 0.5$.

3. The color-flavor-spin factor from the requirement that the 6q's or 6$\bar{q}$'s have the quantum numbers of the S or $\bar{S}$ the totally antisymmetric singlet representation of SU(18): $18 \times 17 \times 16 \times 15 \times 14 \times 13/(6 \times 5 \times 4 \times 3 \times 2)/18^6 = 5.46 \times 10^{-4}$. For the case of the ϕ, the analogous factor is $(1/3)(3/4)(1/9) = 0.028$, where the factors are respectively for forming a color singlet, spin-1 and specified flavor.

Thus ignoring spatial wave-function suppression we get the estimate

$$\text{BR}_{\Upsilon_{2,3S}\to S\bar{\Lambda}\bar{\Lambda}} = 0.008 \left(\frac{0.03}{0.5} \times \frac{5.4 \times 10^{-4}}{2.8 \times 10^{-2}} \right) \text{BR}_{\Upsilon_{2,3S}\to \phi K^+ K^-}$$

$$= 1.25 \times 10^{-11}.$$

Whether there is also a penalty for making pp instead of $K^+ K^-$ is unclear. No such penalization is called for when calculating inclusive S production as in the Appendix of [2], because baryon number conservation requires production of a pair of anti-baryons with S. However for the exclusive amplitude the penalization may apply, since there is no unitarity

Final State	branching fraction	number events
ggg	0.357 ± 0.026	
γgg	0.0097	
Υ_{2S}+anything	0.106	
(non-Υ_{2S})$b\bar{b}$+anything	0.32	
$\ell^+\ell^-$	$\approx 3 \times 0.02$	

TABLE V: Selected Υ_{3S}, from [5]. No non-leptonic non-b-containing final states seen.

sum over all possible final states. In that case, there would be an additional suppression $\mathcal{O}(10^{-1})$ as seen in J/Ψ decay and the heuristic 0.1 for a baryon relative to a meson high-multiplicity hadronic final states. We also dropped the flavor-counting-factor since that is not so significant.

The above analysis indicates that the current exclusive scattering limit on branching fraction is about 4 orders of magnitude above the required level of $\mathcal{O}(10^{-11})$. Can we understand this small value from another point of view? Basically, it follows from the fact that production of any given low-multiplicity exclusive channel in the decay of ggg with invariant mass ≈ 10 GeV is highly suppressed. This can be seen as follows: in $\Upsilon_{1,2,3S}$ decay, respectively 82%, 59% and 36% go through the ggg channel. From the Tables, the largest 3-body channels detected is consistently VM+2 PS, each having branching fraction $\approx 2 \times 10^{-6}$. From this, we can estimate the suppression factor for a ggg with invariant mass ≈ 10 GeV to go to any 3-body exclusive final state is about 10^{-5}. Starting from the inclusive branching fraction estimate 2.7×10^{-7}, we then arrive at the estimated branching fraction for the exclusive channels $\Upsilon_{2,3S} \to S\bar{\Lambda}\bar{\Lambda} + cc$ of few 10^{-12}. Thus two different estimation methods point to the same production level for this exclusive final state, more than 4 orders of magnitude below the current experimental limit.

XIII. FEASIBILITY OF USING $B - S = \pm 4$ AS A DIAGNOSTIC FOR S PRODUCTION

With an estimated inclusive branching fraction of $\approx 3 \times 10^{-7}$ in $\Upsilon(1S, 2S, 3S)$ final states, and few-body exclusive branching fractions typically a factor 10^4 or more smaller than their inclusive counterparts, based on the discussion above, it is motivated to ask whether searching for an excess of events with $B - S = \pm 4$ could be a possible strategy. Or, more generally, comparing the relative abundances of events with B-S combinations that are rare but get contributions from events when an S or $\bar{S}$ is produced and escapes, with its quantum numbers balanced in the remaining hadrons.

A proper study requires detector simulations, but the feasibility can be assessed as done below, taking a single "effective" efficiency e_b for identifying a produced baryon or anti-baryon as such and "effective" efficiency e_s for identifying a produced strangeness+1 or strangeness-1 particle as such.

Final State	branching fraction	number events
$\gamma\,\pi^+\pi^-$	$6.3 \pm 1.2 \pm 1.3 \times 10^{-5}$	
$\gamma\,2\pi^+2\pi^-$	$2.5 \pm 0.7 \pm 0.5 \times 10^{-4}$	26
$\gamma\,\pi^+\pi^-K^+K^-$	$2.9 \pm 0.7 \pm 0.6 \times 10^{-4}$	29
$\gamma\,\pi^+\pi^-p\bar{p}$	$1.5 \pm 0.5 \pm 0.3 \times 10^{-4}$	7 ± 6
$\gamma\,\pi^0\pi^0$	1.7×10^{-5}	
$\gamma\,K^+K^-$	$< 1.14 \times 10^{-5}$	90% CL
$\gamma\,p\bar{p}$	$< 0.6 \times 10^{-5}$	90% CL
$\gamma\,2h^+2h^-$	$7.0 \pm 1.1 \pm 1.0 \times 10^{-4}$	80 ± 12
$\gamma\,3h^+3h^-$	$5.4 \pm 1.5 \pm 1.3 \times 10^{-4}$	80 ± 12
$\gamma\,4h^+4h^-$	$7.4 \pm 2.5 \pm 2.3 \times 10^{-4}$	80 ± 12
$\gamma\,2K^+2K^-$	1.14×10^{-5}	2 ± 2

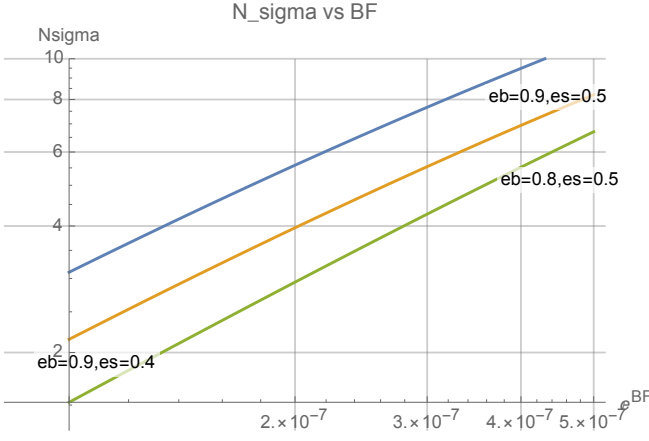TABLE VI: Radiative Υ_{1S}, CLEO measurements from [5]

FIG. 14: Significance as a function of sexaquark branching fraction, for 10^9 $\Upsilon(1S, 2S, 3S)$ decays and different assumed ID efficiencies, from top to bottom $\{e_b, e_s\} = \{0.9, 0.5\}, \{0.9, 0.4\}, \{0.8, 0.5\}$.

The other needed input are f_b, the branching fraction for producing a $B - \bar{B}$ pair in the final state and f_s, the branching fraction for producing a strange-anti-strange pair in the final state. From Z-decay final states, we adopt for our rough estimate $f_b = 0.05$, $f_s = 0.16$. We make the further simplifying assumption that the branching fraction to produce a pair of B's (in the absence of $S, \bar{S}$ production) is f_b^2, an so on. We designate the branching fraction to produce a single S or $\bar{S}$

by g. In the following, we take $g \ll f_b < f_s$ and keep higher orders in f_b and f_s such that the dropped terms are less significant than those kept, assuming e_b, $e_s > 0.2$.

As a simplifying assumption, we take the efficiency of correctly recognizing a $B = +1$ and $B = -1$ particle to be the equal, which is not exactly true, and similarly for strangeness ± 1. For this rough estimate, we track as if ID'ing B and S is independent and uncorrelated, but that is not exact – for instance $\Lambda, \bar{\Lambda}$'s are particularly easy to ID but in the approximation adopted, the efficiency of counting them would be $e_b e_s$, also missing the correlation due to the fact that the geometric penalty should not be counted independently. In fact, for those reasons, the estimate below may be somewhat pessimistic. Likewise, studies focussing specifically on correlations in hyperon production (e.g., excess of events with observed Λ, Λ or $\bar{\Lambda}, \bar{\Lambda}$ compared to expectations from $\Lambda, \bar{\Lambda}$) may prove to be more favorable due to their enhanced ID power, overcoming their more limited statistics.

Using the abbreviation {nxbyBzsvS} to represent the fraction of final states in which there are exactly x identified baryons, y identified anti-baryons, z identified S=+1 particles and v identified S=-1 particles, we can write all of the {nxbyBzsvS}'s up to final states with exactly 4 identified B and/or S non-zero particles. The following gives some examples, now denoting $f_s \to h$; $f_b \to f$ for compactness and denoting baryon (anti-baryon) and strangeness +1 (-1) as b,B,s,S for more compact expressions:

$$n1b = e_b(f(1 - e_b) + 2g(1 - e_b)(1 - e_s)^2 + 2f^2(1 - e_b)^3)(1 + h(1 - e_s)^2) \tag{31}$$

$$n2b2S = e_b^2 e_s^2(g + f^2 h^2(1 - e_b)^2(1 - e_s)^2) \tag{32}$$

$$n1b1B1s1S = e_b^2 e_s^2(fh + 4fh^2(1 - e_s)^2 + 4f^2 h(1 - e_b)^2) . \tag{33}$$

Note that this analysis does not consider mis-identification which must be taken into account for a real assessment, but it does give a useful idea of the possible statistical power.

The most sensitive combination to find a signal for $g \neq 0$ is of course $n2b2S = n2Bn2s$. Fig. 14 shows the signifi-

cance by which a given sexaquark branching fraction is distinguished from background according to this simplified analysis, for $N_{\text{tot}} = 10^9$. The statistical model estimate is BF = $g = 2.7 \times 10^{-7}$ and the significance scales as $\sqrt{N_{\text{tot}}}$. We have defined

$$n_\sigma(g) = \frac{(n2b2S(g) + n2B2s(g) - (n2b2S(g = 0) + n2B2s(g = 0))\sqrt{N_{\text{tot}}}}{\sqrt{(n2b2S(g) + n2B2s(g) + (n2b2S(g = 0) + n2B2s(g = 0))/2}} . \tag{34}$$

The different colored lines give 3 examples of how the significance depends on the efficiencies e_b and e_s. The Belle-II particle ID efficiency for baryon and kaons is 0.8-0.9 depending on how hard they cut, which depends on what backgrounds they want to suppress, so we consider $e_b = 0.8$ and 0.9. Since only

charged K's have a definite strangeness, we penalize kaons by a factor-2; hyperons on the other hand have clearly determined strangeness, so we consider $e_s = 0.4$ and 0.5. Not surprisingly, large e_b is more important than large e_s, since baryons are rarer and thus any sexaquark contribution makes a larger

relative impact on the baryon abundances. A detailed analysis could exploit other combinations such as n2b1S which have some sensitivity to g but with a larger fractional contribution from standard channels, and use cases like n1b1B1s1S which get no contribution from S or $\bar{S}$ to develop confidence that the systematics of the background are fully understood.

The result of the crude analysis given above is roughly applicable for any process in which the multiplicity of gluons and $q\bar{q}$'s produced is large. Thus it could be a guide for the feasibility of heavy ion and a GLUEX search as well.